11-1-2013

Top Quark Working Group Report

Nikolaos Kidonakis
Kennesaw State University, nkidonak@kennesaw.edu

Et. Al.

1

Top quark working group report

Conveners: K. Agashe, R. Erbacher, C. E. Gerber, K. Melnikov, R. Schwienhorst.

Contacts by topic: A. Mitov, M. Vos, S. Wimpenny (top mass); J. Adelman, M. Baumgart, A. Garcia-Bellido. A. Loginov (top couplings); A. Jung, M. Schulze, J. Shelton (kinematics); N. Craig, M. Velasco (rare decays); T. Golling, J. Hubisz, A. Ivanov, M. Perelstein (new particles); S. Chekanov, J. Dolen, J. Pilot, R. Pöschl, B. Tweedie (detector/algorithm).

Contributors: S. Alioli, B. Alvarez-Gonzalez, D. Amidei, T. Andeen, A. Arce, B. Auerbach, A. Avetisyan, M. Backovic, Y. Bai, M. Begel, S. Berge, C. Bernard, C. Bernius, S. Bhattacharya, K. Black, A. Blondel, K. Bloom, T. Bose, J. Boudreau, J. Brau, A. Broggio, G. Brooijmans, E. Brost, R. Calkins, D. Chakraborty, T. Childress, G. Choudalakis, V. Coco, J.S. Conway, C. Degrande, A. Delannoy, F. Deliot, L. Dell'Asta, E. Drueke, B. Dutta, A. Effron, K. Ellis, J. Erdmann, J. Evans, C. Feng, E. Feng, A. Ferroglia, K. Finelli, W. Flanagan, I. Fleck, A. Freitas, F. Garberson, R. Gonzalez Suarez, M. L. Graesser, N. Graf, Z. Greenwood, J. George, C. Group, A. Gurrola, G. Hammad, T. Han, Z. Han, U. Heintz, S. Hoeche, T. Horiguchi, I. Iashvili, A. Ismail, S. Jain, P. Janot, W. Johns, J. Joshi, A. Juste, T. Kamon, C. Kao, Y. Kats, A. Katz, M. Kaur, R. Kehoe, W. Keung, S. Khalil, A. Khanov, A. Kharchilava, N. Kidonakis, C. Kilic, N. Kolev, A. Kotwal, J. Kraus, D. Krohn, M. Kruse, A. Kumar, S. Lee, E. Luiggi, S. Mantry, A. Melo, D. Miller, G. Moortgat-Pick, M. Narain, N. Odell, Y. Oksuzian, M. Oreglia, A. Penin, Y. Peters, C. Pollard, S. Poss, H. B. Prosper S. Rappoccio, S. Redford, M. Reece, F. Rizatdinova, P. Roloff, R. Ruiz, M. Saleem, B. Schoenrock, C. Schwanenberger, T. Schwarz, K. Seidel, E. Shabalina, P. Sheldon, F. Simon, K. Sinha, P. Skands, P. Skubik, G. Sterman, D. Stolarski, J. Strube, J. Stupak, S. Su, M. Tesar, S. Thomas, E. Thompson, P. Tipton, E. Varnes, N. Vignaroli, J. Virzi, M. Vogel, D. Walker, K. Wang, B. Webber, J.D. Wells, S. Westhoff, D. Whiteson, M. Williams, S. Wu, U. Yang, H. Yokoya, H. Yoo, H. Zhang, N. Zhou, H. Zhu, J. Zupan.

1.1 Introduction

The top quark was discovered in 1995 [1, 2] and it is still the heaviest elementary particle known today. Thanks to its large mass, and the related strength of its coupling to the Higgs boson, the top quark may be a key player in understanding the details of electroweak symmetry breaking. Studies of the top quark properties at the Tevatron and Run I of the LHC have given us a detailed understanding of many properties of this particle, including its mass, production and decay mechanisms, electric charge and more. With the exception of the large forward-backward asymmetry in $t\bar{t}$ production that has been observed at the Tevatron, all results on top quark pairs and single top production obtained so far have been consistent with the Standard Model. We note that in this context, the anomaly in the b quark forward-backward asymmetry observed at LEP might get amplified for the much heavier top quark.

In the short and mid-term future, top quark studies will be mainly driven by the LHC experiments. Exploration of top quarks will, however, be an integral part of particle physics studies at any future facility. Future lepton colliders will have a rich top quark physics program which would add to our understanding of this interesting quark. Detailed simulation studies have been carried out for linear electron-positron

machines (ILC and CLIC). First attempts have been made to extrapolate these to the case of a circular machine (TLEP). In this report we describe what can be achieved based on projection studies for the LHC and for future lepton colliders. The report is organized along six topics:

- Measurement of the top quark mass;
- Studies of kinematic distributions of top-like final states;
- Measurements of top quark couplings;
- Searches for rare decays of top quarks;
- Probing physics beyond the Standard Model with top quarks;
- Algorithms and detectors for top quark identification at future facilities.

Main conclusions for each topic are presented in Sect.1.8.

1.2 The top quark mass

The top quark mass is a parameter whose precise value is essential for testing the overall consistency of the Standard Model or models of new physics through precision electroweak fits. The exact value of the top quark mass is also crucial for understanding whether the Standard Model *without further extensions* can be continued to energies compared to the Planck scale, without running into problems with the stability of electroweak vacuum [3]. To put both of these statements into perspective, we note that the value of the top quark mass, as quoted by the Particle Data Group, is $m_t = 173.5 \pm 0.6 \pm 0.8$ GeV. The total uncertainty on m_t is therefore close to 1 GeV; this is the best relative precision available for *any* of the quark masses.

Nevertheless, we know that for precision electroweak fits, a 0.9 GeV uncertainty in the top quark mass corresponds to a 5.4 MeV uncertainty in the W-mass (see e.g. Refs. [4] and [5]). Since the W-mass is expected to be measured with this precision at the LHC, and significant improvements in δM_W beyond this are not likely, we conclude that the future of precision electroweak physics requires the measurement of the top quark mass to at least a precision of less than 0.5 GeV, and desireably to 0.3 GeV so that the top sector is not limiting in EW precision fits.

In addition, the vacuum stability issue depends strongly on the value of the top quark mass. Indeed, as shown in Ref. [3], changing m_t by 2.1 GeV around the central value $m_t = 173.1$ GeV, the energy scale where the Higgs potential becomes unstable changes by *six* orders of magnitude, from $\mu_{\rm neg} \sim 10^8$ GeV to $\mu_{\rm neg} \sim 10^{14}$ GeV! It is easy to estimate that if m_t is known with $0.3 - 0.5$ GeV uncertainty, as required by the electroweak fit, the scale can be estimated much more precisely, to within a factor of five. We conclude that the knowledge of the top quark mass with the 0.5 GeV uncertainty will have an important impact on our understanding of particle physics.

Furthermore, it has recently been suggested [6] that a much more precise measurement of the W mass can be performed at a circular e^+e^- collider such as TLEP, where $\delta M_W \leq 1.5$ MeV can probably be achieved. For the purpose of precision electroweak fits, such high precision can be only utilized if the top quark mass is measured with the matching precision of about 0.1 GeV. As we explain below, this can be accomplished at an e^+e^- collider such as the ILC, CLIC, or TLEP itself. Knowing m_t with such a precision will also allow for a much more decisive tests of the vacuum stability problem in the Standard Model. The interest in testing this scenario may increase greatly if no new physics at the TeV scale is found in the Run II of the LHC.

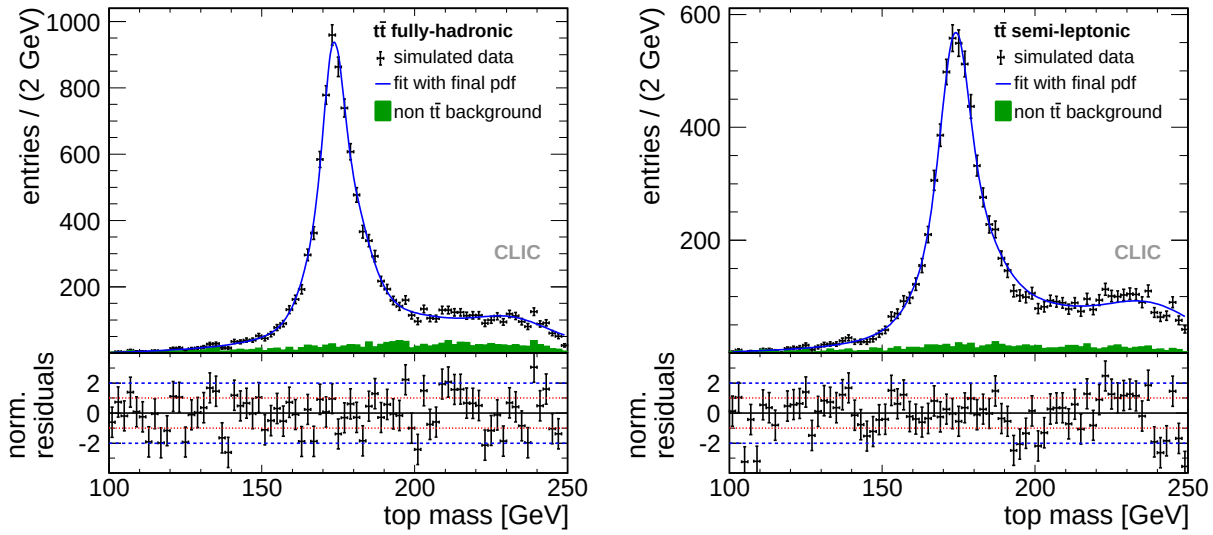

Figure 1-1. *Distribution of reconstructed top mass for events classified as fully-hadronic (left) and semileptonic (right). The data points include signal and background for an integrated luminosity of 100 fb^{-1} [7]. The pure background contribution contained in the global distribution is shown by the green solid histogram. The top mass is determined with an unbinned likelihood fit of this distribution, which is shown by the solid line.*

Note that for these purposes, a numerical value for theoretically well-defined top quark mass parameter, for example $m_t^{\overline{\rm MS}}$, is required.

1.2.1 Linear Colliders

A e^+e^- collider will allow us to study electroweak production of $t\bar{t}$ pairs with no concurring QCD background. Therefore, precise measurements of top quark properties become possible.

The top quark mass can be measured at e^+e^- machines using two complementary methods. First, one can use the invariant mass of the reconstructed bW system from the top decay. The result of a full simulation study at a 500 GeV linear collider [7] (CLIC, with similar results for ILC) is shown in Fig. 1-1. The figure demonstrates also the small residual background expected for top quark studies at any e^+e^- machines. In the second method the top mass is determined in a threshold scan, an option unique to an e^+e^- machine. In the threshold scan the so-called 1S top quark mass can be measured to an experimental precision of better than 40 MeV where studies have shown that the statistical error is dominant. Expressing the measurement in terms of the theoretically well defined $\overline{\rm MS}$ mass will inflate the uncertainty to $\sim$ 100 MeV, as shown in detailed simulations [8, 7, 9] and advanced theoretical computations (see e.g. Ref. [10] and references therein).

We note that with respect to the top quark mass determination, all lepton colliders that were suggested so far perform similarly[1] and that an additional attraction of measuring m_t at a lepton collider is a clean theoretical interpretation of the result of the measurement. As we explain below, the situation is more

[1]We note that some improvements in the m_t determination can be expected at the muon collider and at TLEP thanks to reduced beamstrahlung, although this still has to be demonstrated by detailed simulations.

confusing at a hadron collider, although new methods for m_t measurements developed at the LHC help to mitigate this difference.

1.2.2 Top quark mass at the LHC

As previously noted, a precision of 0.5 GeV or better in the top quark mass is motivated by the future of precision electroweak fits. It is an interesting question whether m_t measurements with such a precision can be accomplished at the LHC. To answer it, we will first make some general remarks about measurements of m_t.

Existing measurements of the top quark mass rely on complex techniques required by the difficult hadron collider environment. The highest accuracy is currently achieved using the so-called matrix-element method (for a recent review, see [11]). We will explain a generic measurement of the top quark mass by considering the following example. Any measurement of the top quark mass is based on fitting a particular piece of data to a theory prediction where m_t enters as a free parameter. Hence, we write

$$D = T(m_t, \alpha_s, \Lambda_{\rm QCD}) = T^{(0)}(m_t) + \frac{\alpha_s}{\pi} T^{(1)}(m_t) + \mathcal{O}(\Lambda_{\rm QCD}/m_t, \alpha_s^2), \tag{1.1}$$

where D on the left hand side is a particular kinematic distribution measured in experiment and T on the right-hand side is a theoretical prediction, expanded in power series in the strong coupling constant. We have indicated in Eq.(1.1) that the selected distribution should be minimally affected by non-perturbative corrections; we will return to this point below. We also note that inclusion of QCD corrections necessitates a clear definition of the renormalization scheme, which then fixes the mass parameter extracted from the fit. Since the two popular choices of the renormalized mass parameter, the pole mass and the $\overline{\rm MS}$ mass, differ by almost 7 GeV, the specification of the renormalization scheme in the extraction of the top quark mass is an important issue. Solving Eq.(1.1), we find the top quark mass m_t. In general, the quality of such a solution depends on the *accuracy* of the theoretical prediction that we have in the right hand side, which is controlled by the order in perturbation theory included there. The majority of current analyses are performed with leading order theoretical tools. This amounts to setting $T^{(1)} \to 0$ in the above equation. The expected error on m_t is then

$$\delta m_t \sim \frac{\alpha_s}{\pi} \frac{T^{(1)}}{T^{(0)'}} \sim \frac{\alpha_s m_t}{\pi} \frac{T^{(1)}}{T^{(0)}} \sim \frac{\alpha_s}{\pi} m_t \sim 6 \text{ GeV}, \tag{1.2}$$

where $T^{(0)'} = {\rm d}T^{(0)}/{\rm d}m_t$ and we used $T^{(0)'} \approx T^{(0)}/m_t$. It is obvious from Eq.(1.2) that the estimated error in Eq.(1.2) is *significantly larger* than the current $\mathcal{O}(1)$ GeV error on m_t. We conclude that if m_t is obtained from a generic distribution at leading order, one can not, in general, expect the accuracy that is better than few GeV. Fortunately, there are two ways to get around this problem. The first one requires inclusion of NLO QCD corrections into a theory prediction; effectively, this pushes the error to $m_t(\alpha_s/\pi)^2 \sim 0.3$ GeV which is acceptable. The second one amounts to finding a kinematic distribution which has a *strong* dependence on m_t; in this case, ${\rm d}T^{(0)}/{\rm d}m \gg T^{(0)}/m_t$ and the estimate in Eq.(1.2) receives an additional suppression.

As we show below, *new* experimental techniques that address the question of the top quark mass determination follow the two approaches described above. The above discussion can be used to argue that *well-established* methods for the top quark mass determination may have additional systematic errors which are not accounted for in their error budgets. Indeed, the matrix element method[2] is designed to maximize probabilities for kinematics of observed events by adjusting values of the top quark mass on an event-by-event basis. It can be thought therefore as an attempt to fit a very large number of kinematic distributions for the

[2]The template method [12] is subject to similar arguments.

	Ref.[13]	Projections				
CM Energy	7 TeV	14 TeV				
Luminosity	$5fb^{-1}$	$100fb^{-1}$		$300fb^{-1}$		$3000fb^{-1}$
Pileup	9.3	19	30	19	30	95
Syst. (GeV)	0.95	0.7	0.7	0.6	0.6	0.6
Stat. (GeV)	0.43	0.04	0.04	0.03	0.03	0.01
Total, GeV	**1.04**	**0.7**	**0.7**	**0.6**	**0.6**	**0.6**

Table 1-1. *Precision of the top quark mass measurements that can be expected using conventional (likelihood-type) methods. Extrapolations are based on the published CMS lepton-plus-jets analysis. An additional* 0.3 GeV *systematic error was added to all extrapolated results.*

best value of m_t. An unsatisfactory feature of this method is its "black-box" nature that does not allow one to understand which kinematic features of the top quark pair production process drive this sensitivity. While such methods – by design – should find distributions that show strong dependence on m_t, it is not clear if the relevant distributions are sensitive to non-perturbative effects whose description from first principles is not possible. Moreover, such approaches routinely rely on the use of parton shower event generators instead of proper QCD theory. This means that Eq.(1.1) becomes

$$D = T(m_t, \alpha_s, \Lambda_{\rm QCD}) \approx T^{(0)}_{\rm MC}(m_t, \alpha_s, \Lambda_{\rm QCD}, \text{tunes}), \tag{1.3}$$

where, as indicated in the last step, additional approximations, including parton shower tunes, are performed on the "theory" side. While the quality of this approximation *for the purpose of determining* m_t may be good, it is simply not clear how to assign the error to the parameter m_t which is extracted following this procedure. To make this problem explicit, the top quark mass extracted from Eq.(1.3) should be properly referred to as the "Monte-Carlo mass ", whose relation to short-distance definition of m_t is not understood.

In spite of the caveats with the top quark mass determination that are inherent to conventional methods, it is interesting to estimate precision in m_t that can be achieved at the LHC. We do that using extrapolations of what has been accomplished at the Tevatron and during the run I of the LHC. In Table 1-1 we show such projections for conventional methods assuming that the mass is measured in the lepton + jet channel for the 14 TeV LHC for different integrated luminosities and pile-up scenarios. We assume the $t\bar{t}$ production cross-section to be $\sigma_{pp\to t\bar{t}} = 167(951)$ pb at 7 and 14 TeV LHC, respectively. It follows from Table 1-1 that conventional methods may, eventually, lead to the measurement of the top quark mass with an error of about 0.6 GeV and that this error is totally dominated by systematic uncertainties. It is interesting to point out that precision in m_t saturates for the integrated luminosity of 300 fb^{-1} and that there is no benefit of using yet higher luminosity for the top quark mass measurement. The reason for this is the increased pile-up and related degradation of the jet energy scale determination in the high-luminosity environment, see a detailed discussion in Section 1.7.1. Note, however, that the systematic error estimate in Table 1-1 includes 0.3 GeV that was added to all extrapolated results to account for unforeseen sources of systematics; if we omit this 0.3 GeV uncertainty, the uncertainty on the top quark mass measurement becomes very small.

Conceptual problems with conventional methods can be mitigated be measuring the top quark mass from well-defined kinematic distributions which, on the one hand, are sufficiently sensitive to m_t and, on the other hand, can be cleanly interpreted in terms of a particular type of the top quark mass. The latter requirement forces us to select kinematic distributions that are infra-red safe, so that their computations in higher-orders of QCD perturbation theory can be performed. In addition, methods for measuring the top quark mass

	Ref.[14]	Projections		
CM Energy	7 TeV	14 TeV		
Luminosity	$5fb^{-1}$	$100fb^{-1}$	$300fb^{-1}$	$3000fb^{-1}$
Syst. (GeV)	1.8	1.0	0.7	0.5
Stat. (GeV)	0.90	0.10	0.05	0.02
Total	**2.0**	**1.0**	**0.7**	**0.5**

Table 1-2. *Projections for the uncertainty in m_t determined using the CMS end-point method [14]. Extrapolations are based on the published CMS analysis.*

should, ideally, be immune to contamination from beyond the Standard Model physics – a scenario that is conceivable if there is top-like BSM physics at the energy scale close to $2m_t$. For example, if m_t is determined from the total cross-section $\sigma_{pp\to t\bar{t}}$ and if the measurement of $pp \to t\bar{t}$ receives unknown contributions from top-like BSM physics, the extracted value of the top quark mass will be smaller than the true m_t. This scenario can occur for example in SUSY models with light stop squarks $m_{\tilde{t}} \sim m_t$ that are still not excluded experimentally (cf. discussion in Section 1.6.1.2).

Methods for top quark mass determination that are based on the analysis of kinematic distributions of top quark decay products are as close to an ideal method as possible. The main reason is that, up to small effects related to selection cuts and combinatorial backgrounds, the kinematic variables involved in the analysis can often be chosen to be Lorentz invariant in which case they decouple the production stage from the decay stage. This minimizes impact of any physics, BSM or SM, related to $t\bar{t}$ production on the top quark mass measurement. Some of these methods are also insensitive to the physics of top quark decay and are entirely driven by energy-momentum conservation. We will describe two of the methods that belong to this category – the "end-point" method developed recently by the CMS collaboration [14] and the "J/ψ'' method suggested long ago in Ref. [15].

The idea of the end-point method is based on the observation that the invariant mass distribution of a lepton and a b-jet contains a relatively sharp edge whose position is correlated with m_t. Therefore, by measuring the position of this end-point, one can determine the top quark mass. The number of events close to the end-point is fitted to a linear combination of a flat background and a linear function $N_{lb} \sim N_{\rm bck} + S(m_{\rm lb} - m_0)$, where m_0 gives the position of the end-point. The attractive feature of this method is that it is (almost) independent of any assumption about the matrix element and that it clearly measures either the pole mass *or* some "kinematic" mass which is close to it. At the small expense of being more model-dependent, one can actually improve on this method by utilizing not *only* the position of the end-point but also the shape of the $m_{\rm lb}$ distribution. Note that away from the kinematic end-point the shape of m_{lb} distribution is accurately predicted through NLO QCD including off-resonance contributions and signal-background interferences [16, 17]. Close to the end-point re-summed predictions are probably required and are not available at present.

Nevertheless, even without potential improvements, the end-point method offers an interesting alternative to conventional methods. Uncertainties in m_t that one may hope to achieve are estimated in Table 1-2. We note that by using the end-point method we *do gain in precision by going to high-luminosity LHC*. Our projections show that the error as small as 0.5 GeV can be reached. The dominant contributions to systematic uncertainty for each of these studies are the jet-energy scale and hadronization uncertainties. Similar to estimates of δm_t that can be achieved using conventional methods, we add 300 MeV to the systematic uncertainty in Table 1-2, to account for unforeseen sources of the systematics.

	Ref. analysis	Projections				
CM Energy	8 TeV	14 TeV			33 TeV	100 TeV
Luminosity	$20fb^{-1}$	$100fb^{-1}$	$300fb^{-1}$	$3000fb^{-1}$	$3000fb^{-1}$	$3000fb^{-1}$
Theory (GeV)	-	1.5	1.5	1.0	1.0	0.6
Stat. (GeV)	7.00	1.8	1.0	0.3	0.1	0.1
Total	**-**	**2.3**	**1.8**	**1.1**	**1.0**	**0.6**

Table 1-3. *Extrapolations of uncertainties in top quark mass measurements that can be obtained with the J/Ψ method.*

Another approach to measuring the top quark mass that is very different from conventional ones is the so-called J/ψ method [15]. Here the top quark mass is obtained from fits to the invariant mass distribution of three leptons from the *exclusive* decays of the top quark $t \to eB \to eJ/\psi X \to eeeX$, where X denotes light hadrons. The extrapolations for the J/ψ-method are shown in Table 1-3. The attractive feature of this approach is its absolute complementarity to more traditional methods discussed above. The uncertainties in case of the J/ψ method are dominated by statistical uncertainties for luminosities below 100 fb^{-1} and by theory uncertainties for higher luminosities. The theory uncertainties in m_t are estimated to be of the order of 1 GeV; they are caused by scale and parton distribution functions uncertainties and by uncertainties in $b \to B$ fragmentation function. Some reduction of theory uncertainties can be expected, although dramatic improvements in our knowledge of the fragmentation function are not very likely. This is reflected in the change of the theory error shown in Table 1-3 for 14 TeV LHC with 3000 fb^{-1} where it is assumed that NNLO QCD computation of the exclusive production of J/ψ in $t\bar{t}$ events will become available and that the scale uncertainty will be reduced by a factor of two.

We note that other methods of measuring m_t with relatively high precision are possible and were, in fact, discussed in the literature. On the experimental side, the three-dimensional template fit method was recently presented by the ATLAS collaboration [18]. The key idea here is to determine the top quark mass, the light-quark jet energy scale and the b-quark jet energy scale from a simultaneous fit to data, thereby transforming a large part of the systematic uncertainty related to jet energy scales to a statistical one. While this measurement determines the "Monte Carlo" mass and the error on this measurement is not competitive with other m_t-determinations at the moment, its key idea can be applied in conjunction with other methods and will, hopefully, help to reduce systematic uncertainties. Another potentially interesting opportunity is provided by the top quark mass measurements based on exploiting m_t-dependence of lepton kinematic distributions. Although such studies were not actively pursued experimentally, they may offer an interesting avenue for the top quark mass measurement in the high-pile-up scenario given their independence of jet energy scale uncertainties. Theoretical studies of some lepton distributions and their sensitivity to m_t were performed through NLO QCD in Ref. [19] with the conclusion that an $\mathcal{O}(1.5)$ GeV error on m_t can be achieved; further studies that include more realistic estimates of uncertainties are clearly warranted. Finally, it was proposed recently to employ $t\bar{t}j$ events to constrain the top quark mass [20]. This method is clean theoretically and appears to be feasibly experimentally; as shown in Ref. [20], an $\mathcal{O}(1)$ GeV uncertainty in m_t can be achieved.

The top quark width of 1.4 GeV is too narrow to be measured directly at the LHC. It can be probed indirectly through single top quark production [21], which can be determined to about 5% at high-luminosity LHC, see Section 1.3. The width can be measured directly to a few percent through a top pair threshold scan at a lepton collider [22, 8].

We conclude by making a general remark about the future of the top quark measurements at a hadron collider. While hadron collider measurements of the top quark mass *cannot* compete with e^+e^- colliders, our discussion shows that it is possible to have a number of top quark measurements at the LHC, including the high-luminosity option, which are clean theoretically and show high sensitivity to m_t. It is also important to stress that these measurements are typically limited by different types of uncertainties, so that combining their results under the assumption that errors are uncorrelated is a reasonable thing to do. A combination of the results of different measurements, that determine theoretically well-defined top quark mass, can lead to further reduction in the error on m_t that is achievable at the LHC, pushing it into a $0.3 - 0.4$ GeV range. Further reduction of the uncertainty in the top quark mass determination is possible at suggested e^+e^- machines (ILC, CLIC, TLEP). Such measurements are important for testing if the Standard Model *without further extensions* can be consistently extrapolated to Planckian energy scales. Interest in such studies should increase if no new physics is found at the Run 2 at the LHC.

1.3 Top quark couplings

The couplings of the top quark to the W and Z bosons, photon, gluon, and the Higgs boson are explored in this section. It is particularly important to make a direct measurement of the top quark-Higgs boson Yukawa coupling. Simple estimates suggest that typical BSM physics at the TeV scale modifies the top quark couplings to gauge bosons at the percent level [23] but, at the same time, larger $\mathcal{O}(10\%)$ shifts are still possible (see also discussion in Section 1.6). Also, our knowledge of the top quark Yukawa coupling is poor at the moment and the direct measurement of this coupling with any precision is very important. Modifications of top quark couplings typically lead to a more complex structure of the interaction vertices, going well beyond simple-minded re-scaling of SM couplings. This creates additional complications and requires us to understand how all the different couplings can be disentangled.

We note that most of the top quark couplings are measured by comparing observed *rates* of relevant processes with SM expectations. This puts stringent requirements on theoretical predictions and experimental control of systematics, making couplings measurements a difficult endeavor at the LHC. This section compares the precision reach of couplings measurements at low-and high-luminosity LHC to that expected at lepton colliders (mainly ILC and CLIC). Higher-energy hadron colliders are not expected to improve the measurements much beyond the LHC sensitivity (except possibly for the $t\bar{t}Z$ coupling) and are thus not studied here. The muon collider allows for the same studies as done at the ILC, but with smaller beam-related uncertainties and higher luminosity. TLEP provides larger data samples than the ILC, though only near the $t\bar{t}$ treshold, and it has insufficient energy to measure Yukawa coupling through direct $t\bar{t}H$ production though it should be able to reach a sensitivity of $\mathcal{O}(30\%)$ to the ttH coupling from a threshold scan. The top quark couplings sensitivity is compared here using the anomalous coupling notation; a related discussion in terms of effective operators can be found in Refs. [24, 25].

1.3.1 Strong interaction

The strong coupling constant of the top quark is fixed in the Standard Model by the requirement of $SU(3)$ color gauge-invariance. The modifications of this coupling can be expected through radiative corrections which may introduce additional structures, such as chromoelectric and chromomagnetic dipole operators in the $gt\bar{t}$ vertex. These modifications occur both in the Standard Model and in models of new physics. For example, the Higgs exchange between top quarks modifies the strength of gluon-top quark interaction in top pair production by $\mathcal{O}(0.5\%)$ while it does not affect the interaction of light quarks to gluons.

Strong interactions of the top quark are studied in top quark pair production, including the $t\bar{t}$+jets processes, both at the Tevatron and the LHC. A summary of the current prediction and measurements is shown in Table 1-4. An experimental uncertainty of about 5% on $\sigma(pp \to t\bar{t})$ has been achieved at the 8 TeV LHC and it is not expected to significantly improve beyond that during further LHC operations. The theory prediction for the total cross-section through NNLO QCD is available [26, 27, 28]; it shows a residual scale uncertainty of about 3.5%, comparable to experimental precision. Note that, at this level of precision, electroweak corrections may be important; indeed, as shown in a recent update [29], the weak corrections to $t\bar{t}$ production at the LHC are close to -2.5%. We conclude that, at a few percent level, there is no indication that strong interactions of top quarks are significantly different from that of light quarks.

More exotic types of modifications of top quark strong interactions, such as chromoelectric d_t and chromomagnetic μ_t dipole moments of top quarks, are better constrained from changes in kinematic distributions. We will discuss this in Section 1.4. Ref. [30] finds that constraints of 1% or below are possible with 100 fb^{-1} at 13 TeV.

Exchanges of axigluons or Kaluza-Klein excitations of gluons not only modify couplings of top quarks to gluons, but also generate four-fermion operators that involve light and heavy quarks $(\bar{q}T^a q)$ $(\bar{t}T^a t)$. These operators can be directly probed at the LHC, where the sensitivity to scales between 1.2 TeV and 3 TeV can be expected [31].

Finally, top quark coupling to gluons can be probed at a linear collider through a threshold scan. The peak cross-section at threshold is proportional to $\sigma_{\rm peak} \sim \alpha_s^3/(m_t\Gamma_t)$. Using the total cross-section and other measurements at threshold, one can determine the strong coupling constant with better than one percent precision and the total width of the top quark Γ_t with the precision of a few percent [8, 7].

	Theory prediction		LHC Measurement	
CM Energy [TeV]	7	8	7	8
Luminosity [fb^{-1}]			1-5	2-15
Top pairs $\sigma(t\bar{t})$ [pb]	172 ± 7 [26]	246 ± 10 [26]	173 ± 10	241 ± 32 (ATLAS) [32]
			(LHC comb.) [33]	227 ± 15 (CMS) [34]
Single top σ(t-chan) [pb]	66 ± 2 [35]	87 ± 3 [35]	83 ± 20 (ATLAS) [36]	95 ± 18 (ATLAS) [37]
			67 ± 6 (CMS) [38]	80 ± 13 (CMS) [39]
Single top $\sigma(Wt)$ [pb]	15.6 ± 1.2 [35]	22.2 ± 1.5 [35]	16.8 ± 5.7 (ATLAS) [40]	27.2 ± 5.8(ATLAS) [41]
			16 ± 4 (CMS) [42]	23.4 ± 5.4 (CMS) [43]

Table 1-4. *LHC single top and top pair production cross-section measurements.*

1.3.2 Weak interactions: W boson

The coupling of the top quark to the W boson is studied in top quark decays and in single top quark production at the LHC and the Tevatron, and in top quark decays at the linear collider. The effective Lagrangian describing the Wtb interaction including operators up to dimension five is [24]

$$\mathcal{L} = -\frac{g}{\sqrt{2}}\bar{b}\gamma^\mu(V_L P_L + V_R P_R)tW_\mu^- - \frac{g}{\sqrt{2}}\bar{b}\frac{i\sigma^{\mu\nu}q_\nu}{M_W}(g_L P_L + g_R P_R)tW_\mu^- + h.c.\,, \tag{1.4}$$

where M_W is the mass of the W boson, q_ν is its four-momentum, $P_{L,R} = (1 \mp \gamma_5)/2$ are the left- (right-) handed projection operators, and V_L is the left-handed coupling, which in the SM is equal to the Cabibbo-Kobayashi-Maskawa matrix element V_{tb} [44]. The right-handed vector coupling V_R and the left-and right-handed tensor couplings g_L and g_R may only appear in the SM through radiative corrections.

The measurement of helicity fractions of W bosons through lepton angular distributions in top quark decays can distinguish SM-like left-handed vector couplings from right-handed vector and from left-or right-handed tensor couplings. With the data collected at the 8 TeV LHC, V_R, g_L and g_R can be constrained to be smaller than 0.1. We note that theoretical predictions for W-boson helicity fractions in the SM have been extended to NNLO QCD [45, 46, 47] and, therefore, theory uncertainties on helicity fractions are about one order of magnitude smaller than experimental one. Measuring the helicity fraction to a similar level at the high-luminosity LHC and beyond is therefore necessary to obtain the best sensitivity to new physics.

Single top quark production involves the tWb vertex in top quark production and thus also provides information on the magnitude of the tWb coupling and the CKM matrix element $|V_{tb}|$. Single top quarks are produced in three different modes: the "t-channel" mode where a W boson is exchanged between a light quark line and a heavy quark line, which has the largest cross-section; the "Wt associated production" mode where either the decay or the exchange of a virtual b quark leads to the final state of a top quark and a W boson, with the next-to-largest cross-section; and the "s-channel" production and decay of a virtual W boson, which has a very small cross-section. The LHC cross-section measurements for t-channel and Wt together with the corresponding prediction are shown in Table 1-4. The three modes have different sensitivities to new physics and anomalous couplings. LHC measurements of single top quark production, in particular in the t-channel mode, are also sensitive to off-diagonal CKM matrix elements [48]. The single top production cross-section measurement already is dominated by systematic uncertainties [36, 38, 40], and the situation is not expected to improve much at higher energies or with larger datasets. The ultimate cross-section uncertainty will likely be around 5%, similar to top pair production, so that uncertainties on tWb coupling and $|V_{tb}|$ will be close to 2.5% [49]. Searches for anomalous couplings in the tWb vertex depend on the ability to separate the signal from both SM single top and from large backgrounds and are less limited by systematic uncertainties. A search for CP violation through an anomalous coupling gives a limit on $Im(g_R)$ [50]. Finally, an extrapolation of the sensitivity to anomalous couplings from single top quark production and decay shows that with 300 fb^{-1} the anomalous couplings as small as 0.01 can be probed.

Electron-positron colliders are expected to do a comparable job in exploring the strength of tWb interaction vertex by considering the cross-section scan of σ_{tbW} cross-section at CM energies between m_t and $2m_t$. It was estimated in Ref. [23] that g_{tWb} can be measured with the precision of about two percent. Among more exotic options is the possibility to study tWb interaction at a γe collider, with a reach of 10^{-1} to 10^{-2} [51]. The reach is about 10^{-3} to 10^{-2} for a LHC-based electron-proton collider with a CM energy of 1.3 TeV [52].

Knowledge of tWb interaction can be used to compute the top quark decay width Γ_t. This can be compared to direct measurements of Γ_t, discussed in Section 1.2.

1.3.3 Electroweak interaction: Z boson and photon

The interaction of the top quark with neutral electroweak gauge bosons has not been studied in detail so far. Indeed, although both the charge of the top quark [53] and the production cross-section of top pair in association with a photon were measured experimentally [54], this does not give us all the information required to fully constrain the $t\bar{t}\gamma$ vertex. The interaction of top quarks with the Z boson has not been measured yet. Similarly to other coupling, a measurement with $\mathcal{O}(10\%)$ precision will be useful for constraining models of

physics beyond the Standard Model. As an example, Section 1.6 discusses compositeness, which would be constrained by a measurement at this precision.

It is challenging, but perhaps not impossible, to probe $t\bar{t}Z$ and $t\bar{t}\gamma$ couplings at the LHC with 10% precision. A lepton collider would provide even higher precision.

A general expression for $t\bar{t}V$, $V = \gamma, Z$ interaction vertex is [23]

$$\Gamma_{\mu}^{ttX} = ie\left\{-\gamma_{\mu}\left((F_{1V}^{X} + F_{2V}^{X}) + \gamma_5 F_{1A}^{X}\right) + \frac{(q-\overline{q})_{\mu}}{2m_t}\left(F_{2V}^{X} - i\gamma_5 F_{2A}^{X}\right)\right\}, \tag{1.5}$$

where X is either a photon ($X = \gamma$) or Z boson ($X = Z$). The couplings F_{1V}^{γ}, F_{1V}^{Z} and F_{1A}^{Z} have tree-level SM values.

The LHC experiments have measured the production of photons in association with top quark pairs, and will measure both the $\gamma + t\bar{t}$ and $Z + t\bar{t}$ cross-sections. However, in both cases, significant kinematic cuts on final state particles are required either to suppress the backgrounds or, in case of photons, to select events where photons are emitted from top quarks rather than from their decay products [55, 56, 23]. Therefore, extracting the top-photon or top-Z coupling from the associated production is difficult; it relies on a detailed theoretical understanding of the production process. This is becoming available thanks to recent studies of $pp \to t\bar{t}\gamma$ and $pp \to t\bar{t}Z$ processes in next-to-leading order in QCD [57, 58, 59, 60]. Single top quark production in association with a Z boson can also be used to study the tZ coupling [61].

Measurements of the $t\bar{t}\gamma$ and $t\bar{t}Z$ couplings with the highest precision can be performed at a linear collider [22]. The two couplings are entangled in the top pair production process. Separating the two couplings requires polarized beams. For the projections in Table 1-5, electron and positron polarizations of 80% and 30%, respectively, are assumed. It follows from Table 1-5 that most of the top quark couplings to the photon and the Z boson can be measured at a linear collider (ILC/CLIC) to a precision that is typically an order of magnitude better than at the LHC. Despite the lack of detailed studies, the precision on the combined coupling accessible at TLEP is expected to be even better than that at the linear collider due to the higher integrated luminosity. However, the lower energy and lack of beam polarization make it impossible to disentangle the γ and Z couplings and the different couplings in Eq. 1.5. Similarly, detailed studies also have not been performed for a muon collider, which provides larger integrated luminosity and smaller beam uncertainties but also challenging backgrounds; thus it is not clear if it will be able to improve on the linear collider measurements.

In summary, although a linear collider will achieve the highest precision in the $t\bar{t}Z$ and $t\bar{t}\gamma$ coupling measurements, it is clear that the LHC – and in particular its high-luminosity phase – will be able to probe these couplings in an interesting precision range where deviations due to generic BSM physics are expected.

1.3.4 Yukawa coupling

The coupling of the top quark to the Higgs boson is of great interest. Since the top quark provides one of the largest contributions to the mass shift of the Higgs boson, any deviation in the $t\bar{t}H$ coupling from its Standard Model value may have far-reaching consequences for the naturalness problem. The coupling of the top quark to the Higgs boson can be measured at the LHC in different final states. It will also be studied in

Collider	LHC		ILC/CLIC
CM Energy [TeV]	14	14	0.5
Luminosity [fb^{-1}]	300	3000	500
SM Couplings			
photon, F_{1V}^{γ} (0.666)	0.042	0.014	0.002
Z boson, F_{1V}^{Z} (0.24)	0.50	0.17	0.003
Z boson, F_{1A}^{Z} (0.6)	0.058	–	0.005
Non-SM couplings			
photon, F_{1A}^{γ}	0.05	–	–
photon, F_{2V}^{γ}	0.037	0.025	0.003
photon, F_{2A}^{γ}	0.017	0.011	0.007
Z boson, F_{2V}^{Z}	0.25	0.17	0.006
Z boson, ReF_{2A}^{Z}	0.35	0.25	0.008
Z boson, ImF_{2A}^{Z}	0.035	0.025	0.015

Table 1-5. *Expected precision of the top quark coupling measurements to the photon and the Z boson at the LHC [62, 31] and the linear collider [22]. Expected magnitude of such couplings in the SM is shown in brackets. Note that the "non-standard model" couplings appear in the Standard Model through radiative corrections; their expected magnitude, therefore, is* 10^{-2}.

detail at lepton colliders. More details on the top Yukawa coupling measurements can be found in the Higgs working group report [63].

The process $pp \to t\bar{t}H$ can be studied in a variety of final states, depending on the top quark decay mode (lepton+jets or dilepton or all-jets) and the Higgs decay mode ($b\bar{b}$, $\gamma\gamma$, WW etc.). Each final state has a its own, typically large, background, mainly from top quark pair production in association with jets or electroweak bosons. The coupling of the top quark to the Higgs boson is extracted from these measurements with relatively large uncertainties of about 20% initially, with an improvement to 10% at the high-luminosity LHC [64, 65, 66, 67, 62, 31]. At the high-luminosity LHC, the $t\bar{t}H$ final state is also a promising channel to measure the muon coupling of the Higgs boson [68], though it is still statistics-limited. Production of $t\bar{t}H$ with Higgs decay to photons is observable at the LHC [31], which allows for a study of the CP structure of the top-Higgs vertex [69].

Better precision in the top-Higgs coupling can be achieved at lepton colliders running at a sufficiently high CM energy and collecting large integrated luminosity. Initial studies focused on a CM energy of 800 GeV where the $t\bar{t}H$ cross-section is largest, however a measurement at 500 GeV is also possible. For the projections in Tab. 1-6, electron and positron polarizations of 80% and 30%, respectively, are used. For the ILC/CLIC, the nominal luminosity for 1 TeV running is assumed, which corresponds to twice the ILC luminosity at 500 GeV. A comparison of the top Yukawa coupling precision expected at different colliders is shown in Table 1-6, from where it follows that a linear collider provides improvements compared to the high-luminosity LHC. It is also possible to measure the Yukawa coupling in a threshold scan that is sensitive to the modification of the $t\bar{t}$ production cross-section through a Higgs exchange. A precision of $\mathcal{O}(30)$% can, perhaps, be achieved in this case. Note that this is the only way to get information on the top Yukawa coupling at TLEP.

Collider	LHC		ILC	ILC	CLIC
CM Energy [TeV]	14	14	0.5	1.0	1.4
Luminosity [fb^{-1}]	300	3000	1000	1000	1500
Top Yukawa coupling κ_t	$(14-15)\%$	$(7-10)\%$	10%	4%	4%

Table 1-6. *Expected precision of the top quark Yukawa coupling measurement expected at the LHC and the linear collider [63]. The range for the LHC precision corresponds to an optimistic scenario where systematic uncertainties are scaled by 1/2 and a conservative scenario where systematic uncertainties remain at the 2013 level [66, 67, 65]. The ILC [22, 70] and CLIC [71] projections assume polarized beams and nominal integrated luminosities.*

1.4 Kinematics of top-like final states

Working with top quarks requires us to understand how they are produced and how they decay. In this section, we discuss what we know about that and what we can learn in the future. While such a discussion is interesting in its own right, it also allows us to understand to what extent deviations from expected behavior of various top quark distributions in different kinematic regimes can be probed at existing and future facilities. In general, after the run I of the LHC and the studies of top quark pair production at the Tevatron, it is fair to say that dynamics of $t\bar{t}$ production is well-understood. The only, but significant, discrepancy that exists is the disagreement between forward-backward asymmetry for top quarks expected in the Standard Model and the measured value of this asymmetry at the Tevatron. Is it possible to clarify the situation with forward-backward asymmetry at the LHC or other future facilities? This is a data-motivated question that we address in this section.

1.4.1 Kinematic distributions in top quark pair production

Our current understanding of top quark pair production in hadron collisions is based on next-to-leading order computations for the fully-differential process $pp \to t\bar{t} \to W^+W^-b\bar{b}$ both within and beyond the narrow width approximation [16, 17, 72, 73]. The comparison of these computations ensures that the narrow width approximation works very well at the LHC unless one moves to extreme kinematic regimes where production of two on-shell top quarks becomes kinematically unfavorable. The success of the narrow width approximation in $t\bar{t}$ production allows us to claim its validity for more complicated processes, such us production of top quark pairs in association with jets [74, 75, 76] or with gauge bosons, that we will discuss in the next Section. Existing theoretical results on top quark pair production will be further improved by extending available results for differential quantities to next-to-next-to-leading order in perturbative QCD. We note that such results for the total cross-section $pp \to t\bar{t}$ were recently obtained [26, 27, 28].

We will now take a closer look at the quality of theoretical description of various kinematic distributions. To this end, we show distributions in the top quark transverse momentum $p_\perp$ in $pp \to t\bar{t}$ at the 14 TeV LHC in Fig. 1.4.1 and indicate the uncertainties in the predictions caused by imperfect knowledge of parton distribution functions and missing higher-order corrections. We estimate the latter by varying renormalization and factorization scales by a factor of two around the fixed value $\mu = m_t$. The computations are performed with MCFM [77]. We see that scale uncertainties dominate and that uncertainties in theory predictions are at the level of 20%.

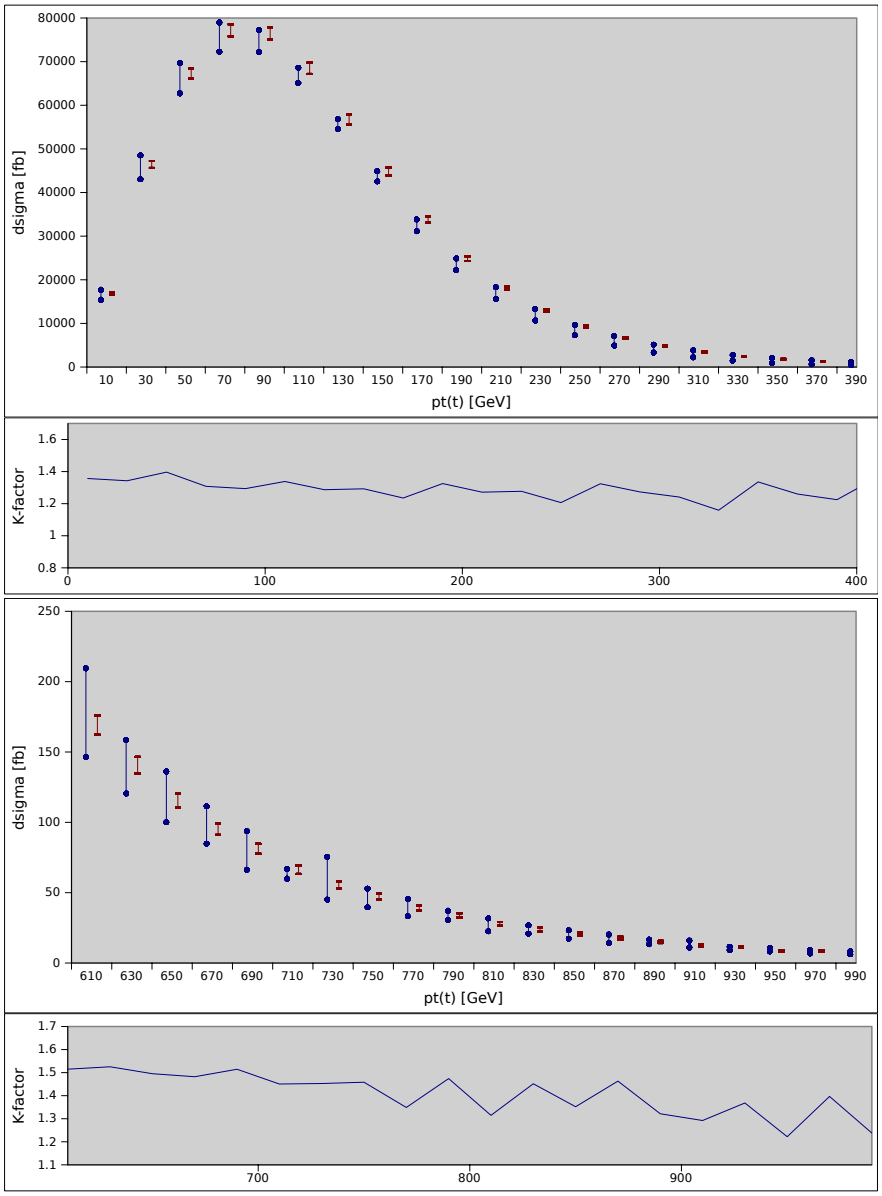

Figure 1-2. *NLO QCD predictions [77] for the transverse momentum of the top quark at the* 14 *TeV LHC. Blue error bars correspond to the central MSTW pdf set and scale variation by a factor of two around* $\mu = m_t$*. Dark red error bands correspond to 1 SD variation of MSTW pdf error sets for fixed renormalization and factorization scale at* $\mu = m_t$*. Note that the red and blue bars can be off-set because at NLO the central scale does not necessarily corresponds to the center of the blue bar. In this case, it seems that it is towards the upper value of the blue bar.*

Another interesting kinematic regime is when each top quark is produced with a high Lorentz boost (¿2), resulting in collimated decay products that may be clustered into a single jet ("boosted" topology). As we will see, it is more difficult to understand the uncertainty in the theoretical prediction for this quantity. Indeed, a MCFM-based computation shows that for $p_\perp > 800$ GeV, the uncertainties on rapidity and $p_\perp$ distributions roughly double compared to the non-boosted regime [78]. However, these uncertainties may be underestimated. Indeed, resummation computations, either traditional or Soft-Collinear Effective Field Theory (SCET). point towards additional positive contributions to $p_\perp$ distributions at high values of the top quark momentum [79, 80]. Forthcoming NNLO computations will be required to resolve this issue.

All kinematic distributions in top quark pair production are routinely checked for signs of new physics. Prominent among them is the distribution in the invariant mass of a $t\bar{t}$ pair, which may be significantly modified by the presence of resonances that decay to top pairs. Theoretical predictions for such distributions exist both in fixed order QCD and in SCET [79]; they show theoretical errors between ten and fifteen percent, depending on $m_{t\bar{t}}$ *and*. Similarly to the $p_\perp$ distribution, these show significant differences between fixed order and resummed results at large values of $m_{t\bar{t}}$.

Other kinematic distributions, such as angular correlations between either top quarks or their decay products, did not lead to studies at the Tevatron because of low statistics. However, such studies at the LHC will become increasingly important as the tool to analyze various subtle features of top quark interactions with with both SM and, hopefully, BSM particles. In the following subsections, we discuss examples of this, considering top quark spin correlations and the forward-backward $t\bar{t}$ asymmetry.

1.4.2 Top quark spin correlations

Spin correlations between t and $\bar{t}$ are an interesting feature of top quark physics, related to the fact that top quark lifetime is so short that $t(\bar{t})$ spin information is transferred to their decay products without being affected by non-perturbative hadronization effects. Observable spin correlations are affected by the structure of $g\bar{t}t$ and tWb interaction vertices. After the observation of top quark spin correlations at the Tevatron [81] and recently at the LHC [82, 83], experimental analyses will soon be able to probe spin correlations in detail. Perhaps, they will use spin correlations as an analysis tool to find and constrain physics beyond the Standard Model.

The cleanest $t\bar{t}$ samples for the study of spin correlations are the ones with two opposite-sign leptons in the final state. Spin correlations in this dilepton mode manifest themselves most prominently in the distribution of the relative azimuthal angle between the two leptons [84]. This distribution is robust under higher order corrections and parton showering effects [72, 85, 86]. For standard acceptance cuts, NLO QCD effects introduce shape changes of at most 20%. If additional cuts are applied that enhance spin correlations, NLO corrections increase the correlation even further. Electroweak corrections have negligible effect and scale variations are small because distributions are typically normalized. On the experimental side, the reconstruction of the lepton opening angle in the laboratory frame is straightforward and can be done with small systematic uncertainties. The normalized azimuthal opening angle distribution is therefore an ideal observable for studying top quark spin correlations. Other observables such as helicity angles, double differential distributions and asymmetries can also be explored.

The utility of top quark spin correlations to search for physics beyond the Standard Model stems from the vector coupling of top quarks to gluons, from the fermion nature of the top quark, and from the couplings of a top quark to a W boson and a b quark through a left-handed vector current. Any changes in that list must lead to an observable change in the spin correlation pattern. For example, it has been shown that top quark spin correlations can be used to distinguish SM top quarks from scalar partners (stops) even if tops and stop

are degenerate in mass [87]. The potential of spin correlations to distinguish SM top pair production and stop ($m_{\tilde{t}} = 200$ GeV) pair production is illustrated in Fig. 1-3 [78].

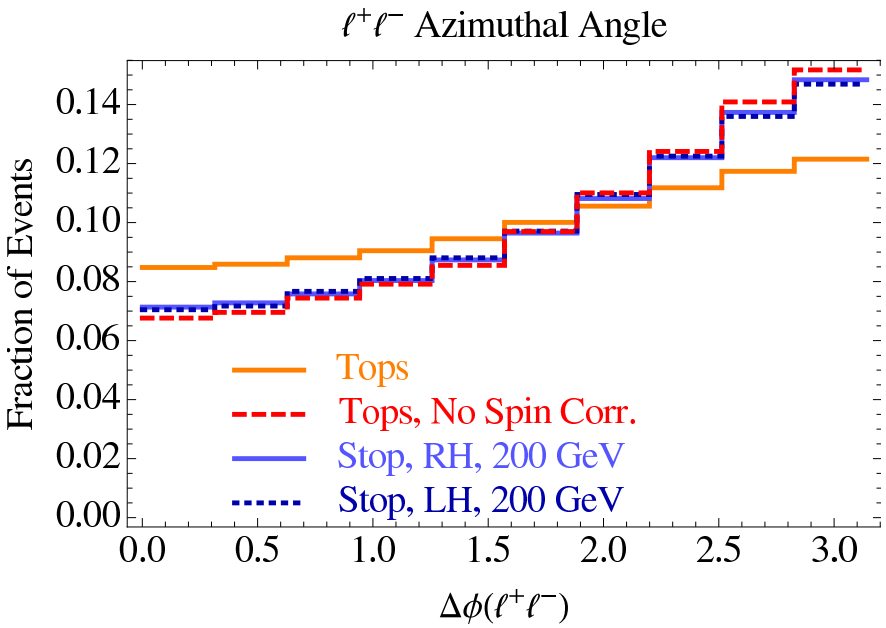

Figure 1-3. *Top quark spin correlation angle for top quark production in the SM and without spin correlation and for stop quark production with different couplings [78].*

Modifications of the $g\bar{t}t$ vertex, that can be parametrized in terms of top quark chromomagnetic $\hat{\mu}_t$ and electric $\hat{d}_t$ dipole moments, can be exposed through spin correlations in the dileptonic and in the semileptonic channels [30, 88]. Here, the magnetic and electric dipole moments $\hat{\mu}_t$ and $\hat{d}_t$ correspond to the Lagrangian $\frac{1}{2}G^a_{\mu\nu}\left(\tilde{\mu}_t\bar{t}\sigma^{\mu\nu}T^a t + \tilde{d}_t\bar{t}i\sigma^{\mu\nu}\gamma_5 t\right)$ where we write $\tilde{\mu}_t = \frac{g_s}{m_t}\hat{\mu}_t$ and $\tilde{d}_t = \frac{g_s}{m_t}\hat{d}_t$. Indeed, using dilepton events sample of the 20 fb^{-1} run at 8 TeV, it should be possible to constrain Re($\hat{\mu}_t$) and Re($\hat{d}_t$) at the few percent level. The imaginary parts Im($\hat{\mu}_t$) and Im($\hat{d}_t$) can be constrained with 15-20% precision from lepton-top helicity angles in the semileptonic channel where a full reconstruction of the $t\bar{t}$ system is possible, using the same dataset. Ref. [30] finds that constraints at the level of one percent or even below are possible with 100 fb^{-1} at 13 TeV. Finally, in case of the discovery of a new resonances which decays into $t\bar{t}$ pairs, top quark spin correlations can also be used to analyze couplings of this new particle [89, 90].

1.4.3 Top quark pair forward-backward asymmetry

Top quark pair production in $q\bar{q}$ collisions exhibits forward-backward asymmetry that arises in higher orders in perturbative QCD [91, 92, 93, 94, 95]. As the result, the top quark is preferentially emitted in the direction of the incoming quark, while the anti-top quark follows the direction of the incoming antiquark. At the Tevatron, the direction of the incoming quark corresponds to the direction of the incoming proton, while the incoming anti-quark most likely comes from an anti-proton. Since LHC is a proton-proton collider, the $t\bar{t}$ asymmetry observation becomes difficult because directions of quark and anti-quark are not correlated with directions of initial hadrons and, in addition, there is a large gluon flux that reduces the asymmetry. The forward-backward asymmetry is measured at the LHC through the difference in rapidity distributions of t

and $\bar{t}$. The harder spectrum of valence quarks in the proton and the correlation of top quark direction with the direction of the incoming quark make the top rapidity distribution broader than the rapidity distribution of the anti-top. The corresponding asymmetry is referred to as the charge asymmetry. It can be written as

$$A_C^\eta = \frac{N(\Delta|\eta| > 0) - N(\Delta|\eta| < 0)}{N(\Delta|\eta| > 0) + N(\Delta|\eta| < 0)} \tag{1.6}$$

where $\Delta|\eta| \equiv |\eta_t| - |\eta_{\bar{t}}|$ tells us whether the reconstructed top or anti-top is more central according to lab-frame *pseudo-rapidity*.

Inclusive forward-backward asymmetries measured at the Tevatron exceed SM predictions by almost three standard deviations [96, 97], with stronger dependence on $t\bar{t}$ invariant mass and rapidity than predicted by the SM. At the LHC, the ATLAS and CMS Collaborations have performed measurements of the charge asymmetry A_C [98, 99] and found agreement with SM predictions. However, these measurements have large errors that makes them not conclusive.

Given that the forward-backward asymmetry is the *only* measurement in top physics that shows profound disagreement with the Standard Model prediction, we feel it is important to understand wether this problem can be resolved. Our estimates for the LHC are presented below. At a linear collider, it is not possible to address this problem directly unless the asymmetry mediator is light and can be directly studied in $e^+e^- \to t\bar{t}jj$.

The higher energy of the 14 TeV LHC increases the fraction of $t\bar{t}$ events that arise from gluon fusion, relative to 7 and 8 TeV LHC. Since $gg \to t\bar{t}$ does not produce an asymmetry, the asymmetric signal decreases with increased center of mass energy of the collider. Already at 7 TeV LHC measurements of the top charge asymmetry are limited by systematic uncertainties. The situation will not change at a higher-energy machine, but higher luminosity can eventually allow us to improve the systematic errors.

SM predictions for the 14 TeV LHC as a function of cuts on the minimum invariant mass of the top pair $m_{t\bar{t}}$ are calculated in Ref. [100]. Cutting on either $t\bar{t}$ invariant mass or center-of-mass rapidity increases the proportion of $q\bar{q}$-initiated top pair events relative to gluon-initiated events, and thus enhances the signal. However, even with kinematic cuts, the size of the signal at the 14 TeV LHC is comparable to the systematic uncertainties on the current measurements. The dominant contributions to the systematic errors are jet energy scale, lepton identification, background modeling ($t\bar{t}$, $W+$ jets, multijets), the model dependence of signal generation and the unfolding procedure. Several contributions to systematic errors, such as jet energy scale and lepton identification, can be reduced with increased luminosity. Possible improvements in background modeling are less clear. The dilepton channel can also be used, usually by defining a lepton-based asymmetry rather than the top quark based A_C, with a sensitivity similar to the lepton+jets one [101, 102].

Our estimates of the ultimate LHC sensitivity [78] show that, with sufficient luminosity, the 14 TEV LHC will be able to *conclusively* measure the SM asymmetry provided that largest systematic errors (background modeling (40%), lepton identification (30%) and $W+$jets modeling (13%) [99]) scale with luminosity. If the asymmetry is enhanced due to BSM effects – as indicated by the Tevatron data – the prospects for observing the asymmetry by CMS and ATLAS become event brighter.

An internal study of the LHCb collaboration [103] concludes that a measurement of the SM $t\bar{t}$ asymmetry by LHCb experiment is possible at the 14 TeV LHC with sufficient luminosity, as suggested earlier in [104]. This will provide a measurement of A_c at the LHC which is complementary to the measurement of A_c by ATLAS and CMS collaborations. Combining all of the measurements, one can probably achieve a significant improvement in the precision compared to individual experiments and hopefully solve the forward-backward asymmetry puzzle.

To this end, note that out of the vast zoology of proposed BSM explanations for the Tevatron anomaly in the top forward-backward asymmetry, axigluons [105, 106, 107] are left looking least constrained after the low-energy LHC run has been completed. Detailed discussions of experimental constraints on axigluon models can be found in [108] for "light" ($M_{G'} < 450$ GeV) axigluons and in [109] for heavy axigluons. The high-luminosity LHC should be able to rule out axigluon models currently under consideration, though it is possible to come up with models that explain the Tevatron asymmetry and are difficult to probe at the LHC.

1.4.4 Other kinematic observables related to A_{FB} at the LHC

The A_{FB} asymmetry is only one of many angular variables whose distributions can be measured in hadron collisions. Indeed, if we consider $t\bar{t}$ production in parton collisions in semileptonic mode, the full kinematics of the event is characterized by 12 angles and the center-of-mass partonic collision energy. In principle, kinematic distributions in these angles describe all kinematic correlations in $t\bar{t}$ events and therefore are sensitive to potential deviations of top couplings to $q\bar{q}$ or gg initial states from their Standard Model values. The forward-backward asymmetry provides an example of this more general framework.

It will be worthwhile to pursue full angular analysis of the $t\bar{t}$ events to understand subtle aspects of top quark pair production or even processes with additional radiation, e.g. $t\bar{t}j$, especially in the context of studying top quark couplings to other Standard Model particles, discussed in Section 1.3. Unfortunately, this general analysis has not been attempted so far. Here, we illustrate this general idea by mentioning additional kinematic observables that can be explored. For example, Refs. [110, 111] introduce two type of additional asymmetries in $t\bar{t}j$ events that can be used to either probe the charge asymmetry or energy asymmetry in a complementary way or to provide additional tools to measure the qg contribution to $t\bar{t}$ production.

1.4.5 Kinematics at the linear collider

At a linear collider, observables such as A^t_{FB} or the slope of the helicity angle λ_t [112] are sensitive to the chiral structure of the $t\bar{t}X$ vertex. A result of a full simulation study of semileptonic $t\bar{t}$ decays [113] is shown in Fig. 1-4.

The figure demonstrates that it will be possible to measure both the production angle θ_{top} of the t quark and the helicity angle θ_{hel} to great precision over a large range, leading to measurements of A^t_{FB} and λ_t with a precision of about 2%. Additionally, the A^t_{FB} and other measurements of the $t\bar{t}$ system, will benefit from a $> 60\%$ pure sample [116] in which to measure the b quark charge. The chiral structures of couplings can be possibly be probed in this way.

Since a significant fraction of top studies will be around the $t\bar{t}$ threshold, understanding kinematic distributions of top quark decay products in this region is important. This is a non-trivial problem that is affected by the need to account for QCD Coulomb interactions to all orders. While results for the total threshold cross-section $e^+e^- \to t\bar{t}$ are currently known through NNLO in QCD [117], similar accuracy for kinematic distributions has not been achieved and it is an interesting and important problem to pursue in the future, if the potential of the threshold scan at the LHC is to be fully exploited.

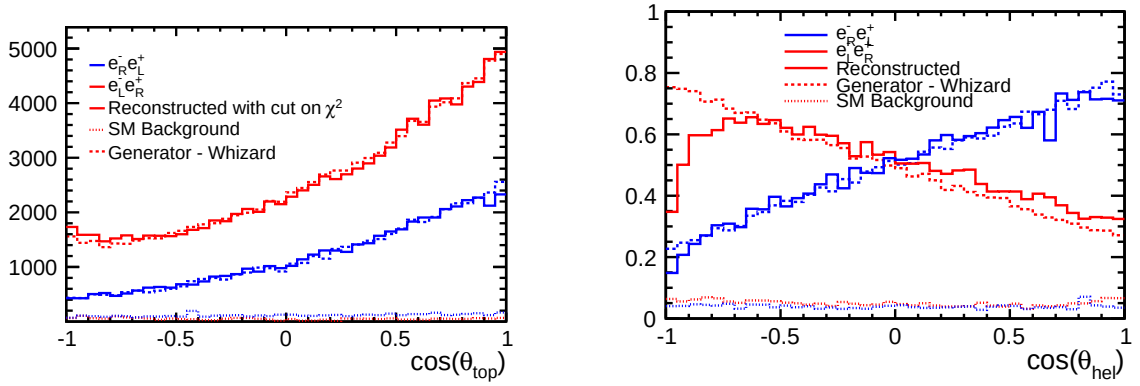

Figure 1-4. *Left: Reconstructed forward backward asymmetry compared with the prediction by the event generator WHIZARD [114, 115]. Right: Polar angle of the decay lepton in the rest frame of the t quark.*

1.5 Rare decays

1.5.1 Introduction

Extensions of the SM often induce sizable flavor-violating couplings between the top quark and other Standard Model particles, typically through new physics in loops. In contrast, flavor-changing neutral couplings of the top are highly suppressed in the SM, so that the measurement of anomalous or flavor-violating couplings of the top quark provides a sensitive probe of physics beyond the Standard Model. Since the top quark decays before hadronizing, top flavor violation is ideally probed through direct flavor-changing neutral current (FCNC) production and decays of the top quark in experiments at the energy frontier. Although flavor-violating couplings of the top may arise from many sources, if the responsible new physics is heavier than the top, it can be integrated out and its effects described by an effective Lagrangian: for details, see, for example, [118].

In Section 1.5.2 we summarize predictions for the size of flavor-changing top decays in the Standard Model and in various motivated models for new physics. In Section 1.5.3 we collect the current best limits on top FCNC decays from direct searches. In Section 1.5.4 we investigate the potential for future measurements at the LHC and ILC to constrain top FCNCs.

1.5.2 Flavor-violating Top Decays

The branching ratio (BR) of a flavor-violating decay of the top quark is given by the ratio of the flavor-violating partial width relative to the dominant top quark partial width, $\Gamma(t \to bW)$. In Table 1-7 we summarize predictions for top FCNC BRs in the Standard Model and various motivated new physics models. In the case of new physics models, the listed BR is intended as an approximate maximal value given ancillary direct and indirect constraints.

Table 1-7. *SM and new physics model predictions for branching ratios of top FCNC decays. The SM predictions are taken from [119], on 2HDM with flavor violating Yukawa couplings [119, 120] (2HDM (FV) column), the 2HDM flavor conserving (FC) case from [121], the MSSM with 1TeV squarks and gluinos from [122], the MSSM for the R-parity violating case from [123, 124], and warped extra dimensions (RS) from [125, 126] .*

Process	SM	2HDM(FV)	2HDM(FC)	MSSM	RPV	RS
$t \to Zu$	7×10^{-17}	–	–	$\leq 10^{-7}$	$\leq 10^{-6}$	–
$t \to Zc$	1×10^{-14}	$\leq 10^{-6}$	$\leq 10^{-10}$	$\leq 10^{-7}$	$\leq 10^{-6}$	$\leq 10^{-5}$
$t \to gu$	4×10^{-14}	–	–	$\leq 10^{-7}$	$\leq 10^{-6}$	–
$t \to gc$	5×10^{-12}	$\leq 10^{-4}$	$\leq 10^{-8}$	$\leq 10^{-7}$	$\leq 10^{-6}$	$\leq 10^{-10}$
$t \to \gamma u$	4×10^{-16}	–	–	$\leq 10^{-8}$	$\leq 10^{-9}$	–
$t \to \gamma c$	5×10^{-14}	$\leq 10^{-7}$	$\leq 10^{-9}$	$\leq 10^{-8}$	$\leq 10^{-9}$	$\leq 10^{-9}$
$t \to hu$	2×10^{-17}	6×10^{-6}	–	$\leq 10^{-5}$	$\leq 10^{-9}$	–
$t \to hc$	3×10^{-15}	2×10^{-3}	$\leq 10^{-5}$	$\leq 10^{-5}$	$\leq 10^{-9}$	$\leq 10^{-4}$

1.5.2.1 SM top FCNCs

SM contributions to top FCNCs are necessarily small, suppressed by both the GIM mechanism and by the large total width of the top quark due to the dominant mode $t \to bW$ [127, 128]. This essentially guarantees that any measurable branching ratio for top FCNC decays is an indication of new physics. The values in Table 1-7 are from the updated numerical evaluation in reference [119]. Note that the results are very sensitive to the value of m_b, since they scale as $m_b(m_t)^4$. The difference between decays involving u quark and c quarks arises from the relative factor $|V_{ub}/V_{cb}|^2$.

1.5.2.2 BSM top FCNCs

Many models for new physics predict new contributions to top FCNCs that are orders of magnitude in excess of SM expectations. Extended electroweak symmetry breaking sectors with two Higgs doublets (2HDM) lead to potentially measurable FCNCs. Parametric expectations are particularly large for 2HDM with tree-level flavor violation, for which flavor-violating couplings between Standard Model fermions and the heavy scalar Higgs H or pseudoscalar A are typically assumed to scale with quark masses, as $\sqrt{m_q m_t / m_W^2}$, in order to remain consistent with limits on light quark FCNCs. The estimates in Table 1-7 are taken from references [129, 120]. The flavor-violating decays arise at one loop due to the exchange of H, A, and the charged Higgs scalar $H^\pm$, with the rate that depends on both the tree-level flavor-violating couplings between fermions and the heavy Higgs bosons and the masses of the heavy Higgs bosons themselves.

Even when tree-level flavor conservation is guaranteed in the 2HDM by discrete symmetries, the model predicts measurable top FCNCs due to loop processes that involve the additional charged Higgs bosons. In this case the rate for flavor-violating processes depends on the mass of the charged Higgs and the angle $\tan\beta$ parameterizing the distribution of vacuum expectation values between the two Higgs doublets. In the Type-I 2HDM, the branching ratios are typically small; the most promising candidate is $t \to gc \sim 10^{-8}$, with rates for $t \to hq$ several orders of magnitude smaller. In the Type-II 2HDM, the leading contribution to $t \to hq$ is enhanced by $\mathcal{O}(\tan^4\beta)$ and may be considerable at large $\tan\beta$. The most optimistic cases are presented in Table 1-7, taken from [121] for Type I and Type II 2HDM. However, given that Higgs coupling measurements

now constrain the allowed range of mixing angles in these 2HDM, the maximal rates for $t \to hq$ consistent with ancillary measurements are likely smaller.

In the MSSM, top FCNCs arise at one loop in the presence of flavor-violating mixing in the soft SUSY-breaking mass matrices. Flavor violation involving the stops is much more weakly constrained by indirect measurements than flavor violation involving light squarks (particularly in the down-squark sector), allowing for potentially large mixing. However, rapidly-advancing limits on direct sparticle production have pushed the mass scale of squarks and gluinos to ≥ 1 TeV, suppressing loop-induced branching ratios. To obtain realistic estimates, in Table 1-7 we extrapolate the results of [122] to the case of $m_{\tilde{g}} \sim m_{\tilde{q}} = 1$ TeV. If R-parity is violated in the MSSM, top decays may also be induced at one loop by baryon (B) or lepton (L) number-violating RPV couplings. The effects of B-violating couplings are larger by an order of magnitude or more. For the estimates in Table 1-7, we extrapolate the results of [123, 124] to $m_{\tilde{q}} = 1$ TeV; for [123] we take their coupling parameter $\Lambda = 1$.

In models of warped extra dimensions, top FCNCs arise when Standard Model fermions propagate in the extra dimension with profiles governed by the corresponding Yukawa couplings. These non-trivial profiles lead to flavor-violating couplings between SM fermions and the Kaluza-Klein (KK) excitations of the SM gauge bosons. Such couplings are largest for the top quark, whose profile typically has the most significant overlap with the gauge KK modes, and lead to flavor-violating couplings that depend on 5D Yukawa couplings and the mass scale of the gauge KK modes. Appreciable flavor-violating couplings involving the top quark and Higgs boson arise from analogous processes involving loops of fermion KK modes.

A possible "Discovery story": it is conceivable that the sensitivity of the LHC and the ILC/CLIC to top FCNCs could lead to the discovery and identification of physics beyond the Standard Model. An intriguing scenario is the observation of the flavor-violating decay $t \to Zc$ at the LHC with a branching ratio on the order of 10^{-5}, at the limit of the projected high-luminosity reach. Such a branching ratio would be some nine orders of magnitude larger than the Standard Model expectation and a clear indication of new physics. At the LHC the primary backgrounds to this channel are Standard Model diboson ZZ and WZ production with additional jets, with a lesser component from Z+jets and rarer SM top processes ttW and ttZ. The diboson backgrounds are fairly well understood and are in excellent agreement with simulations, and even such rare contributions as ttW and ttZ will be well-characterized by the end of the high-luminosity LHC run, making the observation of $t \to Zc$ fairly reliable.

A $t \to Zc$ signal described above is consistent with new physics arising from a variety of models, such as warped extra dimensions, a composite Higgs, or a flavor-violating two-Higgs-doublet model. Ancillary probes of FCNC processes become crucial for validating the signal and identifying its origin. Some of the most important probes that allow differentiation between these options are the rare decays $t \to gc, t \to \gamma c$, and $t \to hc$, which have similar reach at the high-luminosity LHC. In the case of warped extra dimensions or a composite Higgs, the corresponding branching ratios for $t \to gc$ and $t \to \gamma c$ are orders of magnitude below the sensitivity of the LHC, but the branching $t \to hc$ may be as large as 10^{-4}, within the reach of high-luminosity LHC. Thus a signal in $t \to Zc$ with a tentative signal in $t \to hc$ but no other channels would be indicative of warped extra dimensions or a pseudo-Goldstone composite Higgs, see Section 1.6. Such rates would also suggest a relatively low KK scale, so that complementary direct searches for heavy resonances (see Section 1.6) would play a crucial role in testing the consistency of this possibility. In addition, such a KK scale would also lead to up to a 10 % shift in $\bar{t}tZ$ coupling which can be probed at the LHC or the ILC/CLIC (see section 1.3 of this report). In contrast, in flavor-violating two-Higgs-doublet models, a visible $t \to Zc$ signal can be accompanied by comparable signals in $t \to gc$ and $t \to hc$, allowing this scenario to be similarly differentiated.

Complementary information can be provided by the ILC. Projections of the $\sqrt{s} = 500$ GeV ILC with 500 fb^{-1} place its sensitivity to $t \to Zq$ coming from a γ^μ spin structure at the level of 10^{-4}, but sensitivity to

Table 1-8. *Current direct limits on top FCNCs. (*) denotes unofficial limits obtained from public results. The q in the final state denotes sum over $q = u, c$.*

Process	Br Limit	Search	Dataset	Reference
$t \to Zq$	7×10^{-4}	CMS $t\bar{t} \to Wb + Zq \to \ell\nu b + \ell\ell q$	19.5 fb^{-1}, 8 TeV	[130]
$t \to Zq$	7.3×10^{-3}	ATLAS $t\bar{t} \to Wb + Zq \to \ell\nu b + \ell\ell q$	2.1 fb^{-1}, 7 TeV	[137]
$t \to gu$	3.1×10^{-5}	ATLAS $qg \to t \to Wb$	14.2 fb^{-1}, 8 TeV	[131]
$t \to gc$	1.6×10^{-4}	ATLAS $qg \to t \to Wb$	14.2 fb^{-1}, 8 TeV	[131]
$t \to \gamma u$	6.4×10^{-3}	ZEUS $e^{\pm}p \to (t \text{ or } \bar{t}) + X$	474 pb^{-1}, 300 GeV	[134]
$t \to \gamma q$	3.2×10^{-2}	CDF $t\bar{t} \to Wb + \gamma q$	110 pb^{-1}, 1.8 TeV	[132]
$t \to hq$	8.3×10^{-3}	ATLAS $t\bar{t} \to Wb + hq \to \ell\nu b + \gamma\gamma q$	20 fb^{-1}, 8 TeV	[135]
$t \to hq$	2.7×10^{-2}	CMS* $t\bar{t} \to Wb + hq \to \ell\nu b + \ell\ell q X$	5 fb^{-1}, 7 TeV	[136]
$t \to$ invis.	9×10^{-2}	CDF $t\bar{t} \to Wb$	1.9 fb^{-1}, 1.96 TeV	[133]

$t \to Zq$ in single top production from a $\sigma^{\mu\nu}$ structure at $\sim 10^{-5}$. The observation of comparable $t \to Zc$ signals at the LHC and ILC could then favor a $\sigma^{\mu\nu}$ coupling and rule out candidate explanations such as warped extra dimensions.

1.5.3 Current Limits

Limits on various top FCNC decays have progressed rapidly in the LHC era. We summarize the current best limits from direct searches in Table 1-8. CMS places the strongest limit on the decay $t \to Zq$ in the trilepton final state [130] using the full 8 TeV data set. ATLAS sets a sub-leading limit on $t \to Zq$ using a portion of the 7 TeV data set, but also sets the leading limits on $t \to gq$ via a search for s-channel top production [131] using 8 TeV data. The Tevatron still maintains the best limits on some rare processes, in particular $t \to \gamma c$ from Run I [132] and $t \to$ invisible from Run II at CDF [133]. ZEUS maintains the best inferred limit on $t \to \gamma u$ [134]. The Tevatron and HERA limits on $t \to \gamma q$ are expected to be superseded by LHC limits using the $7 \oplus 8$ TeV data set, but to date no official results are available.

The recent discovery of the Higgs allows for limits to be set on $t \to hq$. The ATLAS collaboration sets the current best limit on $t \to hq$ using the diphoton decay of the Higgs with the full $7 \oplus 8$ TeV data set [135]. In [136] a limit was obtained on $t \to hq$ using the 7 TeV CMS multilepton search with 5 fb^{-1} of data, assuming Standard Model branching ratios for a Higgs boson with $m_h = 125$ GeV. Similar limits may be set using the CMS same-sign dilepton search. The CMS multilepton search has recently been updated to $5 \oplus 20$ fb^{-1} of $7 \oplus 8$ TeV data, and now includes b-tagged categories useful for constraining $t \to hq$; an official CMS search for $t \to hq$ using multi-leptons is ongoing.

Indirect limits on top FCNCs may also be set through single top production, D^0 oscillations, and neutron EDM limits. At present these limits are not competitive with direct searches at the LHC for final states involving photons and Z bosons [138], though they are comparable for final states involving h [139].

Table 1-9. *Projected limits on top FCNCs at the LHC and ILC. "Extrap." denotes estimates based on extrapolation as described in the text. For the ILC/CLIC, limits for various tensor couplings (i.e., with $\sigma_{\mu\nu}$ structure) are shown inside ().*

Process	Br Limit	Search	Dataset	Reference
$t \to Zq$	2.2×10^{-4}	ATLAS $t\bar{t} \to Wb + Zq \to \ell\nu b + \ell\ell q$	300 fb^{-1}, 14 TeV	[140]
$t \to Zq$	7×10^{-5}	ATLAS $t\bar{t} \to Wb + Zq \to \ell\nu b + \ell\ell q$	3000 fb^{-1}, 14 TeV	[140]
$t \to Zq$	$5\,(2) \times 10^{-4}$	ILC single top, γ_μ ($\sigma_{\mu\nu}$)	500 fb^{-1}, 250 GeV	Extrap.
$t \to Zq$	$1.5\,(1.1) \times 10^{-4\,(-5)}$	ILC single top, γ_μ ($\sigma_{\mu\nu}$)	500 fb^{-1}, 500 GeV	[141]
$t \to Zq$	$1.6\,(1.7) \times 10^{-3}$	ILC $t\bar{t}$, γ_μ ($\sigma_{\mu\nu}$)	500 fb^{-1}, 500 GeV	[141]
$t \to \gamma q$	8×10^{-5}	ATLAS $t\bar{t} \to Wb + \gamma q$	300 fb^{-1}, 14 TeV	[140]
$t \to \gamma q$	2.5×10^{-5}	ATLAS $t\bar{t} \to Wb + \gamma q$	3000 fb^{-1}, 14 TeV	[140]
$t \to \gamma q$	6×10^{-5}	ILC single top	500 fb^{-1}, 250 GeV	Extrap.
$t \to \gamma q$	6.4×10^{-6}	ILC single top	500 fb^{-1}, 500 GeV	[141]
$t \to \gamma q$	1.0×10^{-4}	ILC $t\bar{t}$	500 fb^{-1}, 500 GeV	[141]
$t \to gu$	4×10^{-6}	ATLAS $qg \to t \to Wb$	300 fb^{-1}, 14 TeV	Extrap.
$t \to gu$	1×10^{-6}	ATLAS $qg \to t \to Wb$	3000 fb^{-1}, 14 TeV	Extrap.
$t \to gc$	1×10^{-5}	ATLAS $qg \to t \to Wb$	300 fb^{-1}, 14 TeV	Extrap.
$t \to gc$	4×10^{-6}	ATLAS $qg \to t \to Wb$	3000 fb^{-1}, 14 TeV	Extrap.
$t \to hq$	2×10^{-3}	LHC $t\bar{t} \to Wb + hq \to \ell\nu b + \ell\ell qX$	300 fb^{-1}, 14 TeV	Extrap.
$t \to hq$	5×10^{-4}	LHC $t\bar{t} \to Wb + hq \to \ell\nu b + \ell\ell qX$	3000 fb^{-1}, 14 TeV	Extrap.
$t \to hq$	5×10^{-4}	LHC $t\bar{t} \to Wb + hq \to \ell\nu b + \gamma\gamma q$	300 fb^{-1}, 14 TeV	Extrap.
$t \to hq$	2×10^{-4}	LHC $t\bar{t} \to Wb + hq \to \ell\nu b + \gamma\gamma q$	3000 fb^{-1}, 14 TeV	Extrap.

1.5.4 Projected Limits

Although current direct limits on flavor-violating top couplings do not appreciably encroach on the parameter space of motivated theories (compare tables 1-7 and 1-8), future colliders should attain meaningful sensitivity (see table 1-9). Here we will focus on the sensitivity of the $\sqrt{s} = 14$ TeV LHC after 300 and 3000 fb^{-1} of integrated luminosity, as well as the ILC operating at $\sqrt{s} = 250$ and the ILC/CLIC at 500 GeV, with 500 fb^{-1} of integrated luminosity. The case of the $\sqrt{s} = 250$ GeV ILC is particularly interesting, since it possesses sensitivity to top FCNCs through single-top production via a photon or Z boson.

1.5.4.1 LHC projections

At present, estimates of future LHC sensitivity to top FCNCs arise from two sources: official projections from the European Strategy Group (ESG) report [140] and approximate extrapolation from current searches at the 7 and 8 TeV LHC based on changes in luminosity, energy, and trigger thresholds. Table 1-9 provides a summary of the projected limits at the 14 TeV LHC with 300 and 3000 fb^{-1} integrated luminosity.

The ATLAS projections for $t \to qZ, \gamma$ are shown in the table. At present there is no public document from CMS with projections for 14 TeV sensitivity, nor are there official projections from either collaboration for $t \to gq$ or $t \to hq$.

Estimates for LHC sensitivity to $t \to gq$ and $t \to hq$ are obtained by an approximate extrapolation from current searches accounting for changes in luminosity, energy, and trigger thresholds. While crude, when applied to $t \to Zq$ this procedure agrees to within $\mathcal{O}(10\%)$ with the official ATLAS ESG projections and so provides a useful benchmark in lieu of detailed study. The $t \to hq$ entries in the table for the multilepton final state are derived from those in [136] by scaling with the luminosity and $t\bar{t}$ production cross-section. This implies a 95% CL limit $\mathrm{Br}(t \to hq) < 2 \times 10^{-3} (5 \times 10^{-4})$ with 300 (3000) fb^{-1} at 14 TeV. Similarly, estimates based on [135] give a sensitivity (95% CL limit) in the $\ell\nu b + \gamma\gamma q$ final state of $\mathrm{Br}(t \to hq) < 5 \times 10^{-4} (2 \times 10^{-4})$ with 300 (3000) fb^{-1} at 14 TeV. The extrapolation of $t \to gq$ is more delicate, since the process under study involves the tgq anomalous coupling in the production mode. Using the results from [142] to extrapolate the observed 7 TeV limit [143] to 14 TeV, we find $\mathrm{Br}(t \to gu) < 4 \times 10^{-6} (1 \times 10^{-6})$ with 300 (3000) fb^{-1} at 14 TeV and $\mathrm{Br}(t \to gc) < 1 \times 10^{-5} (4 \times 10^{-6})$ with 300 (3000) fb^{-1} at 14 TeV.

1.5.4.2 Linear collider (ILC/CLIC) projections

At the ILC/CLIC, sensitivity studies have focused on operation at $\sqrt{s} \geq 500$ GeV in order to probe both $e^+e^- \to t\bar{t}, t \to Xq$ as well as the single top process $e^+e^- \to tq$ due to, e.g., tZq or $t\gamma q$ anomalous vertices[3]. Linear collider performance at $\sqrt{s} \geq 500$ GeV is studied in some detail in [141], which forms the basis for sensitivity estimates quoted here. The study [141] includes 95% CL estimates for various polarization options, including 80% e^- polarization and 45% e^+ polarization, which are close to the polarization parameters planned for the ILC. In what follows we quote the 80%/45% polarization sensitivity, with the difference between 45% e^+ polarization and 30% e^+ polarization expected to lead to a small effect. We rescale the results of [141] to 500 fb^{-1} to match the anticipated ILC/CLIC integrated luminosity; the results are presented in Table 1-9. Based on these estimates, ILC/CLIC sensitivity at $\sqrt{s} = 500$ GeV should be comparable to LHC sensitivity with 3 ab^{-1} for $t \to Zq$ and $t \to \gamma q$. Since much of the sensitivity comes from single top production, the ILC/CLIC is less likely to provide comparable sensitivity to $t \to hq$ and $t \to gq$.

The ILC also provides sensitivity to tZq and $t\gamma q$ anomalous couplings at $\sqrt{s} = 250$ GeV through single top production via the s-channel exchange of a photon or Z boson, $e^+e^- \to t\bar{c} + \bar{t}c$. In fact, production via Z exchange through the γ_μ vertex reaches its maximal cross-section around 250 GeV and falls with increasing center-of-mass energy. Single top production cross-sections through γ exchange or Z exchange through the $\sigma_{\mu\nu}$ coupling grow with increasing energy but are still appreciable at $\sqrt{s} = 250$ GeV . The disadvantage of $\sqrt{s} = 250$ GeV relative to higher center-of-mass energies is primarily the larger SM backgrounds to the single-top final state. *In any event, this provides an intriguing opportunity for the ILC to probe new physics in the top sector even when operating below the $t\bar{t}$ threshold.*

The prospects for constraining tZq and $t\gamma q$ anomalous couplings at $\sqrt{s} = 250$ GeV have not been extensively studied, but we may extrapolate sensitivity reasonably well based on the results of [144]. To obtain an estimate, we rescale the signal cross-section

after cuts for $e^+e^- \to t\bar{c} + \bar{t}c$ via anomalous couplings at $\sqrt{s} = 192$ GeV in [144] to $\sqrt{s} = 250$ GeV and conservatively assume the background cross-sections are similar between $\sqrt{s} = 192$ GeV and $\sqrt{s} = 250$ GeV. In actuality, the backgrounds should decrease with increasing center-of-mass energy. We assume a 60% b-tag efficiency and arrive at 95% CL estimates in Table 1-9.

[3] As mentioned in section 1.3, TLEP has larger $t\bar{t}$ samples, but no polarization so that separating couplings to γ from those to Z will be difficult.

1.5.5 Vts and Vtd

The measurement of the ratio of top decays with b-tagging to all top decays is sensitive to the off-diagonal CKM matrix elements V_{ts} and V_{td} [145]. A measurement of this ratio at the sub-percent level should be possible at the high-luminosity LHC. The rapidity of the top quark in t-channel single top quark production is also sensitive to V_{ts} and V_{td} [146]. The ultimate precision in V_{ts} and V_{td} will come from a combination of the two methods [48]. Systematic uncertainties and their correlations between different measurements will be a limiting factor, but a precision of better than 0.05 in $|V_{ts}|$ and $|V_{td}|$ should be achievable based on current studies.

1.5.6 Summary

Various well-motivated models predict branching ratios for top FCNC decays starting at $\sim 10^{-4} - 10^{-5}$, with the most promising signals arising in two-Higgs-doublet models and various theories with warped extra dimensions. At present the LHC sensitivity to top FCNC decays is somewhat below the level predicted by motivated theories, with the notable exception of $t \to gu$ where searches for resonant single top production yield a limit $\mathcal{O}(10^{-4})$. However, future colliders, such as the 14 TeV LHC and $\sqrt{s} = 250$ ILC or 500 ILC/CLIC, provide meaningful sensitivity to flavor-violating couplings of the top quark, of the same order as the largest rates predicted in motivated theories. The LHC and the ILC/CLIC can be complementary in this regard: while the sensitivities in tqZ/γ are (roughly) comparable for the two colliders, the LHC is better for gluon couplings, but the ILC/CLIC is the way to go for probing the spin-structure of couplings. Intriguingly, even at $\sqrt{s} = 250$ GeV the ILC should provide sensitivity to $t \to Zq, \gamma q$ that is comparable to that of the high-luminosity LHC. Finally, going from LHC to HL-LHC can improve reach by roughly a factor of two (in rates).

1.6 Searches for new particles associated with the top quark

The top quark provides a sensitive probe for physics beyond the Standard Model, based on the following argument: the presence of new physics at the TeV scale is very well-motivated by its role in solving the Planck-weak hierarchy problem of the SM. Namely, such new particles can prevent quantum corrections from dragging the Higgs boson mass (and hence its vev, i.e., the weak scale) all the way up to Planck scale. Such new particles must then necessarily couple to the Higgs boson. However, because the top quark has the largest coupling (among SM particles) to the Higgs boson, quantum corrections due to the top quark are the dominant source of destabilization of the weak scale. Thus, such new particles typically also couple preferentially to the top quark (among the other SM particles).

In this section, we focus on the *direct* production of such new particles, followed by their decay into top-like final states. In most solutions to the Planck-weak problem, there are actually charge +2/3, colored NP which accomplish the job of canceling the divergence from top quark loop in the Higgs mass (and thus directly stabilizing the weak scale). These can be scalar/spin-0, i.e., stops in supersymmetry (SUSY: see review in [147]). Alternatively, they can be fermionic (often denoted by "top-partners"), as realized in little Higgs (see reviews in [148, 149]) and composite Higgs (accompanied by composite top) models. The latter are conjectured to be dual to the framework of a warped extra dimension, following the AdS/CFT correspondence: see reviews in [150, 151]). The composite Higgs and top (or extra dimensional) models often also contain bosonic $t\bar{t}$ resonances.

With the above motivation, the studies performed for the Snowmass process can be grouped into the following three categories: searches for stops, top-partners and $t\bar{t}$ resonances. These are described in turn below. Note that virtual/indirect effects of such new particles also lead to rare/flavor changing neutral current decays of the top quark which are discussed in section 1.5 of this report. In addition, there can be shifts in couplings of the top quark which already exist in the SM (for example, flavor-preserving ones), as discussed in section 1.3 of this report. Finally, these studies overlap with the work of the Snowmass Beyond Standard Model group, where further examples of New Physics related to top quarks can be found [152].

To illustrate an impact that top physics studies can have on discovering and understanding physics beyond the Standard Model, we now describe a **discovery story**. Here the tell-tale signs for top and Higgs compositeness at the TeV scale is provided by a multitude of measurements and observations in top physics [150, 151]. In particular, suppose there is an observation of a shift in the $t\bar{t}Z$ cross-section of the order of 10% at a linear collider and, possibly even at the HL-LHC (see Section 1.3). It could be a "smoking-gun" signal for this scenario, since this model predicts such a size for this shift (as compared to weakly coupled theories such as SUSY, where this effect is signficiantly suppressed and gives no signal at the LHC). At the same time, in composite models rare decays $t \to cZ$ or $t \to ch$ can occur with a branching fraction of up to 10^{-4} which would then be accessible at the LHC and a lepton collider, see Section 1.5. Finally, both top-partners and $t\bar{t}$ resonances with O(TeV) masses are omnipresent in the compositeness scenario and would thus be accessible at the LHC, and especially its high-luminosity option, via direct production. Therefore, as our story illustrates, top quark physics at the LHC and at a linear collider may be a crucial element of discovering and elucidating physics beyond the Standard Model.

1.6.1 Stops

SUSY is perhaps the most popular solution to the Planck-weak hierarchy problem of the SM. It involves addition of a *superpartner* for every particle of the SM, with a spin differing by 1/2-unit from that of the corresponding SM particle. While, in general, superpartner masses in SUSY models are very model-dependent, naturalness strongly suggests that the scalar partners of the top quark, or *stops*, should have masses around the week scale. The reason is that (as mentioned above) the stops cancel the largest divergence in the Higgs mass squared parameter, coming from the SM top loop. This makes stops a prime target for LHC searches. The results of such searches are typically presented in terms of the "vanilla stop" simplified model, which contains two particles, a stop $\tilde{t}$ and a neutralino LSP $\tilde{\chi}^0$ (i.e., superpartner of photon and Z or Higgs boson). The stop is assumed to decay via $\tilde{t} \to t\tilde{\chi}^0$ with a 100% branching ratio. Within this model, the current "generic" bound on the stop mass is about 700 GeV [153, 154]. One of the tasks of future experiments is to improve the reach on $m(\tilde{t})$ for generic spectra. In fact, both ATLAS and CMS have presented estimates of the discovery reach of LHC-14 and HL-LHC in the vanilla stop model, extrapolating the present 1-lepton search [140, 155]. For a "generic" spectrum, stops up to approximately 800 (900) GeV can be discovered, at a 5-σ level, with 300 fb^{-1} (3 ab^{-1}) integrated luminosity. It is interesting to determine if the reach at LHC 14 TeV for this generic case can be extended beyond the above ATLAS/CMS projections using *special* techniques developed recently and so far applied only to the LHC 7/8 TeV. The first study (as part of the Snowmass process) mentioned below is along these lines.

Moreover, it must be emphasized that lighter stops are still allowed by LHC 7/8 TeV. In particular:

(a) If $m(\tilde{\chi}^0) > 250$ GeV, stops of any mass are allowed;

(b) in the "off-shell top" region, $m_t > m(\tilde{t}) - m(\tilde{\chi}^0) > m_W$, stops above 300 GeV are allowed;

Collider	Energy	Luminosity	Cross Section	Mass
LHC8	8 TeV	20.5 fb^{-1}	10 fb	650 GeV
LHC	14 TeV	300 fb^{-1}	3.5 fb	1 TeV
HL LHC	14 TeV	3 ab^{-1}	1.1 fb	1.2 TeV
HE LHC	33 TeV	3 ab^{-1}	91 ab	3.0 TeV
VLHC	100 TeV	1 ab^{-1}	200 ab	5.7 TeV

Table 1-10. *Stop production mass limits. The first line gives the current bound on stops. The remaining lines give the estimated 5 σ reach, based on a study for the Snowmass process, in stop pair production cross-section and mass for different future hadron collider runs.*

(c) in the "compressed" region, $m(\tilde{t}) \approx m(\tilde{\chi}^0) + m_t$, stops of any mass are allowed (this includes the particularly challenging "stealthy" region, $m(\tilde{t}) \approx m(t) \gg m(\tilde{\chi}^0)$); and

(d) in the "squeezed" region, $m(\tilde{t}) - m(\tilde{\chi}^0) < m_W$, stops of any mass are allowed.

In all of these regions, the kinematics of stop production and decay yields events with little missing transverse energy (MET), reducing the efficiency of LHC searches. Thus, another goal of future experiments should be to explore the special regions listed above. A couple of studies to cover the stealth stops of case (c) above were done as part of Snowmass process and are outlined below.

Although LHC will clearly play a leading role in the generic case[4], it should be emphasized that in any of the special regions, stops can still be within the kinematic reach of the ILC/CLIC, at $\sqrt{s} = 500$ GeV or 1 TeV. In this case, the ILC could play a crucial role in discovering the stops and precisely determining/confirming their properties, *e.g.* spin and masses.

Finally, *addition* of particles (such as gluino or chargino, i.e., superpartners of SM gluon or W) to the above simplified model is well-motivated. Adding such particles to the model generally weakens the exclusion limits. Studies along these lines were also performed for the Snowmass process and are described below.

1.6.1.1 Vanilla stops

Here fully hadronic decays using strategies inspired by [156, 157, 158, 159] are considered. The fully hadronic channel has two advantages over leptonic searches. The first is that it has the largest branching fraction for the top decays. The second is that it has no inherent missing energy from neutrinos, so all the missing energy comes from the neutralinos. This allows many backgrounds to be reduced by vetoing events with leptons. Jet-substructure based top tagging (see section 1.7 of this report) is used to distinguish signal from background. The results are summarized in table 1-10: for more details, see reference [160].

1.6.1.2 Stealth stops

In the above-mentioned ATLAS/CMS projections of reach for stops at LHC 14 TeV, significant gaps in the coverage remain: for example, no discovery is possible for the LSP mass above 500 GeV, as well as in the

[4]direct production of stops at the ILC in this region is not possible, given the current bounds

Collider	Luminosity	Technique	Mass reach
LHC 14 TeV	100 fb^{-1}	spin-correlations	175–200 GeV (for stealth stops, statistical uncertainty only)
LHC 14 TeV	100 fb^{-1}	dileptonic m_{T2}	175–185 GeV and 195-200 GeV (for stealth tops)
LHC 14 TeV	300 fb^{-1}	VBF	400 GeV (for compressed case, with $m(\tilde{t}) - m(\tilde{\chi}^0) = 10$ GeV)

Table 1-11. *Estimated 5 σ discovery reach for stealth/compressed stops, based on various studies for the Snowmass process. See the text for explanation of these concepts.*

compressed and stealthy regions, even at HL-LHC. It is clear that novel search strategies will be needed to cover these regions.

Two studies of such strategies were contributed to our working group (see table 1-11 for summary of results). Reference [161] focused on the stealthy stop region, which is particularly challenging since, unlike the region with a heavy neutralino, no significant MET is generated even in the presence of ISR jets. The challenge is to distinguish $\tilde{t}\tilde{t}^*$ events from a much larger $t\bar{t}$ background. Two methods to achieve this task have been studied: (a) using spin correlations, which are present in $t\bar{t}$ but not in $\tilde{t}\tilde{t}^*$ events, due to $\tilde{t}$ being a scalar particle [87] (see also section 1.4.2 of this report); and (b) using an m_{T2} cut in dileptonic event sample [162]. It was found that, using spin correlations, LHC-14 with 100 fb^{-1} of data will be able to discover the stealthy stop at the 5σ level, assuming the stop mass of up to 200 GeV and considering statistical errors only. Assuming a 15% systematic error, the m_{T2} method will be able to discover right-handed stealthy stops *except* in the $(185, 195)$ GeV window. The sensitivity to the left-handed stop is poor, since there is no m_{T2} tail in the signal in this case.

The second study [163] analyzed the possibility of using the vector boson fusion stop production channel, which provides additional jets that could be used to tag events with stealthy, compressed, or light stops. For compressed stops with $\Delta M = m(\tilde{t}) - m(\tilde{\chi}^0) = 10$ GeV, it was found that the LHC-14 with 300 fb^{-1} of data will be able to probe $m(\tilde{t}) = 400$ GeV at a 5σ level. The mass reach increases for larger ΔM. Studies for stops in the stealthy, "off-shell top", and "squeezed" regions using vector boson fusion are ongoing.

1.6.1.3 Gluino-initiated stop production

In addition to stops, naturalness also strongly motivates a light gluino, constraining its mass through the one-loop QCD correction to stop mass. A rough naturalness bound is $m(\tilde{g}) < 2m(\tilde{t})$ [164]. This motivates considering a simplified model with gluino, stop and an LSP, with a decay $\tilde{g} \to t\bar{t}$+MET. Assuming that this decay proceeds via an off-shell stop and has a 100% branching ratio, LHC-8 searches rule out gluino masses up to about 1.3 TeV, provided that the LSP mass is below 500 GeV [165, 166]. Extrapolating the search in the all-hadronic channel, CMS estimates a 5σ discovery reach of 1.7 TeV at LHC-14 with 300 fb^{-1} of data [155]. For gluino masses above TeV, boosted tops become increasingly common in $\tilde{g}$ decays, and can be used to tag SUSY events [167] (see section 1.7 of this report for techniques to identify boosted tops). A preliminary study (with no detector simulation) in reference [168] suggests that a search using top tags, in combination with more traditional kinematic cuts in all-hadronic channel, at the LHC-14 with 300 fb^{-1} (3 ab^{-1}) of data will be able to discover gluinos up to 1.8 (2.1) TeV, provided that the stop mass is below 1.1 (1.4) TeV.

Collider	Luminosity	Mass
LHC 14 TeV	300 fb^{-1}	1.8 TeV
LHC 14 TeV	3000 fb^{-1}	2.1 TeV

Table 1-12. *Estimated 5 σ discovery reach for gluino decaying into stops, with R-parity conservation, based on a study for the Snowmass process.*

Collider	Luminosity	Technique/channel	Mass
LHC 14 TeV	300 fb^{-1}	topness, asymmetric	1 TeV
LHC 14 TeV	3000 fb^{-1}	topness, asymmetric	1.3 TeV
LHC 14 TeV	300 fb^{-1}	dilepton, well-tempered neutralino	700 GeV$^{\text{preliminary}}$

Table 1-13. *Estimated 5 σ discovery reach for stops decaying into chargino, based on various studies for the Snowmass process. See the text for explanation of these concepts.*

1.6.1.4 Including more electroweak particles

Another well-motivated extension of the vanilla stop simplified model is to add a chargino $\tilde{\chi}^{\pm}$, with $m(\tilde{\chi}^{\pm}) < m(\tilde{t})$. This is also motivated by naturalness, since the charged Higgsino mass is controlled by the μ parameter which cannot be far above 100 GeV in natural SUSY models [164]. This simplified model has the possibility of *asymmetric* stop events: *e.g.* $pp \to \tilde{t}\tilde{t}^*, \tilde{t} \to t\tilde{\chi}^0, \tilde{t}^* \to b\tilde{\chi}^{\pm}$. A study of the LHC sensitivity to this signal was performed: for details, see reference [169]. The proposed search uses the 1-lepton+MET channel, and relies crucially on the "topness" variable, introduced in [170] as a general tool to suppress the $t\bar{t}$ background in this channel. It was found that 5σ discovery is possible at LHC-14 with 300 fb^{-1} for stop masses up to about 1 TeV, if $m(\tilde{\chi}^0)$ is below about 400 GeV. With 3000 fb^{-1}, the discovery reach extends to stop masses about 1.3 TeV for similar $\tilde{\chi}^0$.

A related simplified model was used in the study in reference [171]. Motivated by the "well-tempered neutralino" dark matter scenario [172], this study considered a spectrum with light bino and Higgsino, leading to three neutralino and one chargino states at the bottom of the SUSY spectrum. It was assumed that all these states are lighter than the stop. The analysis focused on the dilepton signature, where the leptons can come either from top decays or from $\chi^0_{2,3} \to Z\chi^0_1$. It was found that the reach is about 700 GeV.

1.6.1.5 *R*-parity violation

Yet another interesting scenario is *R*-parity violating (RPV) supersymmetry, where decay modes are modified relative to the above cases of *R*-parity conservation. For example, a stop can decay via $\tilde{t} \to \bar{b}\bar{s}$ induced by the UDD superpotential operator. This scenario emerges naturally from models with minimal flavor violation [173, 174]. Direct stop production in this case yields all-hadronic final states, but it might still be possible to search in this channel: see, for example, the Snowmass study [175]. However, just as in conventional SUSY, naturalness strongly suggests the presence of relatively light gluinos. Gluino decays via cascades involving stops, $\tilde{g} \to \tilde{t}t, \tilde{t} \to 2j$, may be observable, even though they do not produce large MET. If $\tilde{g}$ is Majorana, as in simplest SUSY models, such decays can provide a striking same-sign dilepton (SSDL) signature. Current SSDL searches already rule out gluinos up to 800 GeV, independent of the stop mass, in the RPV scenario [176]. At LHC-14 with 300 fb^{-1} (3 ab^{-1}) of data, the projected 5 σ reach of this search in gluino mass is 1.4 (1.6 − 1.75) TeV, depending on the stop mass [177]. These estimates include fast

Collider	Luminosity	Technique	Reach
LHC 14 TeV	300 fb^{-1}	same-sign dilepton	1.4 TeV
LHC 14 TeV	3000 fb^{-1}	same-sign dilepton	1.6–1.75 TeV
LHC 14 TeV	300 fb^{-1}	single-lepton, reconstruct mass	2 TeV $^{\text{preliminary}}$

Table 1-14. *Estimated 5 σ reach for gluino decaying into stops, with R-parity violation, based on various studies for the Snowmass process. See the text for explanation of these concepts.*

detector simulation with Delphes [178], but no pile-up. It also includes an improvement in sensitivity due to an additional requirement of one or two massive jets. The massive jets can be either due to boosted stop decays, or to accidental mergers of neighboring jets in a high jet multiplicity signal event. An alternative approach is a search in a single-lepton channel, which has a higher rate and applies to both Majorana and Dirac gluinos [179]. In this case, the requirement of stop mass reconstruction from jet pairs can be used as an additional handle to suppress backgrounds. At the 14 TeV LHC, this search will be sensitive to *Dirac* gluino masses up to about 2 TeV [180].

1.6.2 Top-partners

As mentioned above, in non-SUSY solutions to the Planck-weak hierarchy problem, the divergence in Higgs mass squared parameter from SM top loop is canceled by new *fermions* which are vector-like under the SM gauge symmetries. Typically, they are color triplets with electric charge 2/3 (i.e., same as the SM top and hence these new particles are dubbed top-partners. Such particles can also arise in other extensions of the SM, so it is useful to follow a model-independent, simplified approach in studying their signals. The top-partners can be produced via QCD interactions in pairs or singly [181], the latter resulting from coupling of top-partner to SM top/bottom, as needed to cancel the SM top divergence in Higgs mass squared parameter.

Based on the $SU(2)_L$ gauge symmetry of the SM, the top-partners are often accompanied by "bottom-partners". Finally, in some composite Higgs models, an extension of the EW symmetry group (from that in the SM) is motivated by the goal of avoiding constrains from $Zb\bar{b}$ [182]: this results in the appearance of color triplet, but charge 5/3 particles (in addition to the above top/bottom partners).

In short, there are three types of vector-like quarks which are well-motivated extensions of the SM, namely, top and bottom-partners and charge-5/3 fermions. Once produced, these vector-like quarks can decay into a top-like final state. All of these cases were studied for various LHC scenarios as part of the Snowmass process (including both single and pair production of top-partners mentioned above) and are discussed below. Note that the current (LHC 7/8 TeV) bound on these quarks is at least 800 GeV [183, 184] so that their direct production at the ILC is not possible.

The single production mechanisms have larger rates than those of pair productions for *heavier* top/bottom partners. Moreover, analyses of single-production channels might permit the measurement of the the couplings of top-partners to the SM top/bottom quark (which were mentioned towards the end of the first paragraph of this section). Note that the top-partner single-production, that proceeds via the intermediate exchange of a bottom quark, has a rate significantly higher than those for a single bottom partner or a charge-5/3 partner, which are mediated by the exchange of a top. Hence, in the following, for bottom partners and charge 5/3 quarks, only pair production is considered. All samples used for the top-partner studies were processed with the Delphes [178] fast detector simulation, using the generic Snowmass detector parameters [185]. The background samples were generated in bins of H_T, as described in [186, 187].

Pair production of top-partners: The top-partner has three possible decay modes: bW, tH and Zt. The interesting feature is that, in the limit of a heavy top-partner, the decay modes are equally shared by these three modes (following the principle of Goldstone equivalence). A general analysis such that the three branching fractions bW, tH, and Zt are free parameters, subject to the constraint that they add up to unity and span a "triangle" of branching fractions, has been performed recently [183]. However, it is useful to consider a nominal set of branching fractions, one that is motivated by naturalness with BF($T \to Wb$) = 0.5, BF($T \to th$) = BF($T \to Zt$) = 0.25. The results from an analysis [183] based on lepton+jets and multi-lepton signatures for all decay modes bW, tH and Zt, and utilizing presence of multiple b-jets, large number of jets, are given in table 1-15. Due to the large mass of the top-partner, jet substructure techniques are utilized to identify the W-tagged and top-tagged jets and to keep the signal yield high and fully optimize the signal-to-background discrimination. Reference [188] contains more details of the analysis.

Single production of top/bottom-partners: As mentioned above, the top-partner can decay into one of three possible final states: ht, Zt and Wb. Since the $W+$ jet backgrounds are considerable for the third mode, here the focus is on the first two decay modes. The basic idea is to reconstruct the top-partner mass using the full event information in the decays $ht \to b\bar{b}\ell\nu b$ and $Zt \to \ell\ell\ell\nu b$. The results are summarized in Table 1-15, for more details, see reference [189].

Pair production of bottom-partners: The decays of bottom-partners can be into W^-t, Zb, or Hb. Thus, pair production of bottom partners can lead to interesting signal of same-sign dileptons via $W^-tW^+\bar{t} \to b\bar{b}\ 2\ W^+\ 2W^-$, followed by leptonic decays of both W^+ (or W^-). More details of this study can be found in reference [190]; here, only the final results, obtained using the nominal branching fractions BF($B \to Wt$) = 0.5, BF($B \to Zb$) = BF($B \to Hb$)= 0.25, are shown in Table 1-15.

Pair production of Charge-5/3 fermion: The charge-5/3 vector-like fermions ($T_{5/3}$) [191] decay via $T_{5/3} \to tW^+ \to bW^+W^+$ and thus the pair production of these particles results in same-sign dileptons with a branching fraction of approximately 0.2. These final states can be distinguished from Standard Model backgrounds with same-sign dileptons by the presence of jets or leptons from the second $T_{5/3}$ and by the magnitude of the scalar sum of transverse momenta of the decay products. At $T_{5/3}$ masses of interest, hadronically W bosons and top quarks from the $T_{5/3}$ decay are often highly boosted and can be identified using the tagging methods described in Section 1.7.2 which enhance the background discrimination. Furthermore, it is possible to fully reconstruct the second $T_{5/3}$, in case of fully hadronic decay, and compute its mass. Table 1-15 displays the reach for these exotic quarks; for more details, see reference[192].

1.6.3 $t\bar{t}$ resonances

As mentioned earlier, in non-supersymmetric solutions to the Planck-weak hierarchy problem, there are typically bosonic new particles which decay dominantly into $t\bar{t}$. Examples are leptophobic Z''s in topcolor models [193] or KK gluons in warped extra dimensional frameworks (conjectured to be dual 4D composite Higgs models: see reviews in [150, 151]). Moreover, such $t\bar{t}$ resonances are favored to be rather heavy (a few TeV) due to the constraints from various precision tests. and/or by the current direct bounds from LHC 7/8 TeV [194, 195, 196, 197]. Thus, the top quarks resulting from their decays are boosted so that the top decay products can be quite collimated, requiring special identification techniques which have been developed recently (for more details, see section 1.7 of this report). In some models, these $t\bar{t}$ resonances can also be broad, thereby adding to the challenge of searching for them.

Three such studies of discovery of $t\bar{t}$ resonances were done as part of the Snowmass process and are discussed in what follows. Of course, post-discovery, the focus will shift to determination of the quantum numbers of these $t\bar{t}$ resonances. For example, the spin and chiral structure of couplings of these resonances can be

Collider	Luminosity	Pileup	3σ evidence	5σ discovery	95% CL
top-partner pair production					
LHC 14 TeV	300 fb^{-1}	50	1340 GeV	1200 GeV	1450 GeV
LHC 14 TeV	3 ab^{-1}	140	1580 GeV	1450 GeV	1740 GeV
LHC 33 TeV	3 ab^{-1}	140	2750 GeV	2400 GeV	3200 GeV
top-partner single production					
LHC 14 TeV	300 fb^{-1}	50	1275 GeV	1150 GeV	
LHC 14 TeV	3 ab^{-1}	140	1130 GeV	1000 GeV	
LHC 33 TeV	3 ab^{-1}	140	1350 GeV	1220 GeV	
LHC 100 TeV	3 ab^{-1}	50	1750 GeV	1600 GeV	
LHC 100 TeV	3 ab^{-1}	140	1750 GeV	1575 GeV	
bottom-partner pair production					
LHC 14 TeV	300 fb^{-1}	50	1210 GeV	1080 GeV	1330 GeV
LHC 14 TeV	3 ab^{-1}	140	1490 GeV	1330 GeV	>1500 GeV
LHC 33 TeV	300 fb^{-1}	50	$>$ 1500 GeV	$>$ 1500 GeV	$>$ 1500 GeV
Charge 5/3 fermion pair production					
LHC 14 TeV	300 fb^{-1}	50	1.51 TeV	1.39 TeV	1.57 TeV
LHC 14 TeV	3 ab^{-1}	140	1.66 TeV	1.55 TeV	1.76 TeV
LHC 33 TeV	3 ab^{-1}	140	2.50 TeV	2.35 TeV	2.69 TeV

Table 1-15. *Expected mass sensitivity for heavy top and bottom partners, based on various studies for the Snowmass process.*

measured via angular distribution and polarization of the resulting top quarks: see, for example, references [198, 199, 89]. Finally, note that given the mass range of these $t\bar{t}$ resonances, ILC/CLIC would not play a role in a direct search.

1.6.3.1 Dileptonic

One of the studies (reference [200]) focused on W's from both top quarks decaying into lepton (called "dileptonic" $t\bar{t}$). One expects hadronic activity near the leptons, since the boost of the top quark can put a lepton and a b-jet into the same cone. So, SM $t\bar{t}$ background can be suppressed by in fact requiring *smaller* separation between lepton and the closest jet. The results are summarized in Table 1-16.

1.6.3.2 Semileptonic and fully hadronic

Alternatively, one of the two W's from the decays of the top quarks can give a lepton, while the other one decays into hadrons (semileptonic $t\bar{t}$) or none of the two W's decays into leptons (fully hadronic $t\bar{t}$). A study for the Snowmass process of the fully hadronic channel utilized b-tagging and large-R jet substructure to distinguish jets from boosted top quarks from jets from QCD multijet production, and evaluated the prospects for a search for narrow resonances. The results are expressed in terms of both a leptophobic

Collider	Luminosity	Pileup	95 % exclusion	5 σ discovery
LHC 14 TeV	300 fb^{-1}	50	4.4 TeV	2.8 TeV
LHC 14 TeV	3 ab^{-1}	140	4.7 TeV	4.1 TeV

Table 1-16. *Expected mass sensitivity for a Z' decaying into* dileptonic *$t\bar{t}$, based on a study for the Snowmass process.*

Collider	Luminosity	Pileup	95 % exclusion for Z'	95 % exclusion for KK graviton[5]
LHC 14 TeV	300 fb^{-1}	50	3.7 TeV	2 TeV
LHC 14 TeV	3 ab^{-1}	140	4.1 TeV	2.8 TeV

Table 1-17. *Expected mass sensitivity for a leptophbic Z' and KK graviton decaying into fully hadronic $t\bar{t}$, based on a study for the Snowmass process.*

Z' and KK graviton in warped extra dimensional models: see tables 1-17 and for details, see sections 3.2 and 3.3.2 of reference [201]. The study for Snowmass process of the semileptonic channel is still to be completed and so the results shown in 1-18 (for leptophobic Z' and KK gluon) are from the ATLAS Snowmass whitepaper [140].

Another study focused on the KK gluon (which is typically a *broad* resonance) in warped extra dimensional models. In order to identify boosted top quarks, it used the Template Overlap Method (TOM) [202]. TOM has been extensively studied in the past in the context of theoretical studies of boosted tops and boosted Higgs decays [203], as well as used by the ATLAS collaboration for a boosted resonance search [196]. The method is designed to match the energy distribution of a boosted jet to the parton-level configuration of a boosted top decay, with all kinematic constraints taken into account. Low susceptibility to intermediate levels of pileup (i.e. 20 interactions per bunch crossing), makes TOM particularly attractive for boosted top analyses at the LHC. For more details about how the TOM is used in this study, see section 3.4 of reference [201]: the results are shown in Table 1-19.

1.6.3.3 Single-top resonance

Resonances can appear not only in top pair production, but also in single top quark production. This final state is particularly sensitive to a high-mass W' boson that couples primarily to quarks. Current limits for W' production are around 1.8 TeV [204, 205, 206]. A Snowmass study shows that the reach for W' can be extended to 5 TeV (6 TeV) with 300 fb^{-1} (3000 fb^{-1}) at the 14 TeV LHC [207].

In warped extra dimensional models, the KK gluon discussed in the previous section can also have a sub-dominant decay into $t\bar{c}$ (and $\bar{t}c$) [208]. This process is also relevant for the flavor sector, see the chapter on Flavor working group report [209]. The final state has a single top quark, just like $W' \to tb$, but now the other quark jet is from a charm quark rather than a bottom quark. This has consequences for the b-tag multiplicity and background suppression. The Snowmass study finds a mass limit on the KK gluon of about 3.5 TeV if the branching ratio to tc is 20%. If this branching ratio is less than 5%, the signal is buried below backgrounds and no limit can be set.

A fourth-generation quark with chromomagnetic couplings will be visible in the single top plus W boson final state [210, 211]. Due to the strong nature of the fourth-generation bottom quark production process, the reach for this particle at the high-luminosity LHC should be multi-TeV, similar to the W'.

Collider	Luminosity	Pileup	95 % exclusion for Z'	95 % exclusion for KK gluon
LHC 14 TeV	300 fb^{-1}	50	3.3 TeV	4.3 TeV
LHC 14 TeV	3 ab^{-1}	140	5.5 TeV	6.7 TeV

Table 1-18. *Expected mass sensitivity for a leptophobic Z' and KK* gluon *decaying into* semi*leptonic $t\bar{t}$ [140].*

Collider	Luminosity	Pileup	3 σ evidence	5 σ discovery
LHC 14 TeV	300 fb^{-1}	50	3.8 TeV	3.2 TeV
LHC 14 TeV	3 ab^{-1}	50	4.4 TeV	3.5 TeV

Table 1-19. *Expected mass sensitivity for a KK gluon decaying into semileptonic $t\bar{t}$, based on a study for the Snowmass process using the template overlap method.*

1.7 Top Algorithms and Detectors

Studies of top quarks at future colliders will, in many cases, require dealing with new environments. These include the increased number of pile-up events per bunch crossing in the high-luminosity phase of the LHC, and an increasing reliance on boosted techniques for top identification as the higher energy of the LHC and stronger constraints on scale of BSM physics will require exploration of higher invariant mass events in top quark pair production. In this section we discuss how existing algorithms for top quark studies fare in these cases, and whether or not physics studies that we described in the preceding sections are in fact viable given difficult experimental environments of future colliders. We find that the largest gains from high-luminosity running will be made by taking advantage of boosted top identification algorithms, and by using jet grooming techniques, both of which look promising even in high pile-up environments. We also discuss the unique experimental conditions of the linear collider for top quark studies.

1.7.1 Top quark identification at low transverse momentum

Many of the top quarks produced at the LHC have low transverse momenta, where $p_\perp$ is in the range $25-50$ GeV. Measurements of the total and differential $t\bar{t}$ cross-sections (Sections 1.4 and 1.3), of the top-quark mass (Section 1.2), charge asymmetry (Section 1.4), and single-top measurements (Section 1.3) all require precise and efficient reconstruction of top quarks at low transverse momenta. Top-quark reconstruction at low transverse energies is limited by a number of factors that determine total systematic uncertainty, including: a) jet-energy scale uncertainty which typically accounts for 50% of the overall uncertainty in traditional top-quark measurements based on jets; b) jet-energy resolution uncertainty; c) b-tagging efficiency uncertainty and mistag rates; and d) uncertainty on missing transverse-energy reconstruction. This indicates that progress in precision top measurements that involve jet reconstruction at low $p_\perp$ will require a better understanding of low-p_T jets and $b-$tagging.

The high-luminosity upgrade of the LHC will have an important impact on low-$p_\perp$ top physics. In the current design, we expect more than 100 pileup events per bunch crossing, which will have a negative impact on many final-state observables, particularly on low-p_T jets and b-tagged jets due to their large associated systematics. Studies of this scenario [212] were performed for pp collisions at a center-of-mass energy of $\sqrt{s} = 14$ TeV using a fast detector simulation based on the Delphes 3.08 framework [213]. Jets are

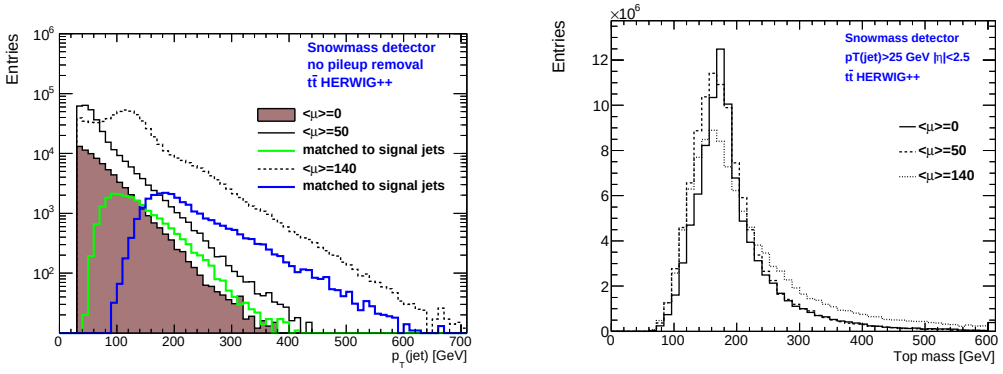

(a) (b)

Figure 1-5. *(a) Plots of jet p_T distributions for different pileup scenarios using the* Delphes *simulation. Also shown are only the jets matched to the top quarks in the event for each pileup scenario, demonstrating the large effect of additional pileup events on top quark reconstruction. (b) Reconstructed top quark masses from trijets by requiring at least four jets with $p_T > 25$ GeV and $|\eta| < 2.5$, and at least one of the jets must be tagged by a b-tagging algorithm.*

reconstructed at the LHC using the anti-k_T algorithm [214] with distance parameter $R = 0.4$ (ATLAS) and $R = 0.5$ (CMS and Snowmass-specific studies). These high-luminosity MC simulation studies showed that, in general, pileup events deposit energy in many calorimeter cells and hence shift the raw jet transverse energies by approximately 50 (120) GeV for 50 (140) pileup events, adding about one additional GeV for each pileup event. This energy needs to be subtracted jet-by-jet using average energies deposited elsewhere in the calorimeter. Tracking in jet reconstruction is also useful, not only to refine the jet energy measurement but also to mitigate the impact of pileup. Nevertheless, the subtraction of pileup results in smeared jet transverse momenta. In addition, there will be many low-p_T fake jets created from pileup events. While tracking can be used to address some of these issues as well, pileup also creates many additional tracks that need to be separated from the tracks belonging to each jet in an event.

Figure 1-5(a) shows the effect of different pileup scenarios on the jet p_T distribution. One consequence of the energy shift is that for the selection of top quark signal jets, pileup subtraction techniques will likely correct energies of the signal jets by 200-400%, leading to larger uncertainties compared to previous analyses. Uncertainties due to pileup will become dominant, and are expected to increase by a factor of two or more at the highest LHC luminosity. As an example, a 2% jet-energy scale uncertainty for a jet measurement without pileup translates to a 3%(5%) uncertainty in case of 50 (140) pileup events scenario.

Since uncertainties in jet resolution, jet energy scales, and b-tagging are dominant uncertainties in many measurements related to top quarks, it is to be expected that precision of such measurements will not improve at higher luminosities and will deteriorate unless new jet energy calibration methods are adopted. While data-driven techniques are likely to improve the assessment of the jet energy scale, it is unlikely that this can make a significant difference to the above conclusion. As the result, the standard top mass measurements do not improve at the high-luminosity phase of the LHC. It should be noted, however, that new techniques which are less reliant on precise knowledge of jet energies will be able to take advantage of the high statistics of the high-luminosity LHC, as we discuss in Section 1.2.

The reconstruction of the top quark mass that is used in many other top quark analyses will also be degraded by the high pileup in high-luminosity runs. A Delphes MC study shows that using the trijet mass for top-

reconstruction is strongly affected by pileup events even when particle-flow methods and pile-up subtraction techniques are used to mitigate the problem [212]. Figure 1-5(b) shows the reconstructed top mass using a procedure similar to the one discussed in [215]. It was also observed [212] that the trijet mass for top-reconstruction strongly depends on top transverse momentum p_T due to large jet multiplicity from ISR/FSR. For p_T >700 GeV, the peak position is at 400 GeV, assuming the same transverse momentum cuts as for low-p_T measurements. This may limit our ability to identify top quarks at such large p_T using the traditional low-energy approaches.

Runs at high pileup will also affect other top physics measurements, such as $t(\bar{t})$+jets and associated top production (such as $Ht\bar{t}$), discussed in Section 1.3, as well as searches for new physics that require a good understanding of low-p_T top quarks, for example searches for rare top decays (Section 1.5). Indeed, low-p_T top quarks require the reconstruction of jets with transverse momentum $30-100$ GeV, which are exactly the jets that are difficult to correct for pileup effects. However, for rare decays or other counting measurements, it may not be so necessary to determine jet energy scales as precisely as measurements using kinematic shapes, so the advantage of the large statistics may very well dominate. Nevertheless, these measurements will be affected by the reduced performance of b-tagging at high pileup, so work will be needed in this area compared to existing algorithms.

In conclusion, we find that the high-luminosity pp collision runs at 14 TeV with more than hundred pile-up events are unfavorable for high-precision top quark measurements based on jets with transverse momenta below 100 GeV. This conclusion will affect $t\bar{t}$ measurements with top quarks produced near threshold that rely on precise knowledge of jet energies, but will affect rate-dependent measurements to a lesser extent, especially with improvements in b-tagging algorithms. We believe that a combination of multiple measurements by CMS and ATLAS may lead to a reduction of systematic uncertainties even in the high pile-up environment.

As will be discussed below, the high-luminosity LHC runs will affect studies of high-p_T(top) top quarks to a lesser extent. It is therefore important to discuss the future of boosted top measurements, where additional reconstruction techniques can be utilized.

1.7.2 Methods particular to boosted top quarks

As we explained in Section 1.6, top quarks play a very important role in many searches for new particles at the highest energies. We find that current algorithms for top quark identification at high-p_T can lead to performance that is similar to what is achieved in current experiments, provided that some modifications to the reconstruction methods are implemented or detectors upgrades are performed.

The decay products of a top quark with high p_T are sufficiently collimated to be reconstructed within a single jet. This happens above ~ 400 GeV for jets with $R = 0.8$. Figure 1-6 shows the evolution of jet mass with the jet transverse momentum for the $t\bar{t}$ process. Because all of the top decay products fall within a single jet, specialized techniques involving jet substructure are required [216, 217]. Semileptonic top decay reconstructions must introduce modified isolation criteria when the lepton starts to overlap with the b quark jet from the top decay. This reconstruction of the top mass within a single jet itself is a good discriminant between boosted top quarks and the overwhelming background from QCD jet production. For example, a recent study [80] has shown that a signal of boosted hadronic top quarks from a Z' boson decay can be observed in the jet mass distribution alone for jets with $p_T > 800$ GeV. Discrimination can possibly be improved further with the addition of b-tagging. The reconstruction of the top jet through its proximity to the mass of the top is the basic idea behind the boosted top studies. In addition, further signal/background separation is achieved by using specialized algorithms that split the top jet into sub-jets, and then examine

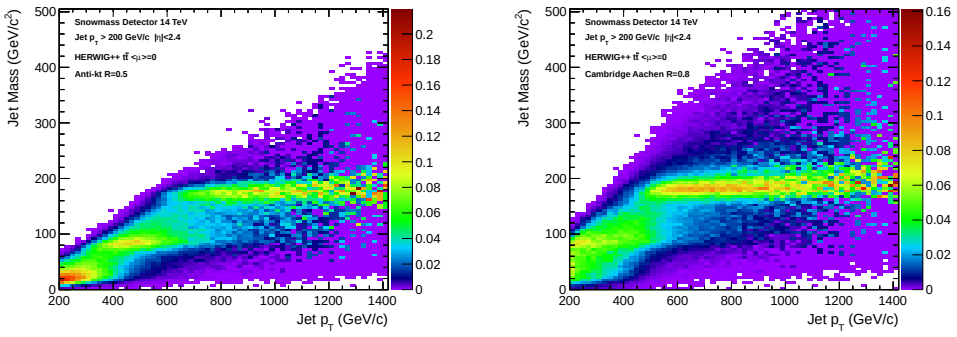

(a) Anti-kt R=0.5

(b) Cambridge Aachen R=0.8

Figure 1-6. *Jet mass vs jet transverse momenta in the* DELPHES *fast simulation for pp collisions at* 14 *TeV for different jet algorithms. The jet transverse spectrum has been reweighed to be flat.*

those to determine if observed jet substructure is consistent with soft and collinear QCD radiation or with the decay of a heavy object into jets through a point-like interaction vertex.

Jet grooming. Boosted jets are affected by pileup just like the unboosted ones discussed in Section 1.7.1. Several algorithms, collectively known as jet grooming algorithms, attempt to mitigate the effect of pileup on jet observables, such as jet mass, by removing soft and wide-angle constituents of jets. The effect of three different jet grooming algorithms have been studied: pruning [218, 219], trimming [220], and filtering [221]. The application of these jet grooming algorithms results in a jet mass distribution that is relatively stable as the number of pileup events increases. Additionally, the jet grooming procedures significantly reduce the masses of QCD jets, enhancing signal/background discrimination significantly.

Substructure and jet shapes. Jet substructure and jet shapes are often discussed as a useful tool for the identification of top quarks and for reduction of the overwhelming rate from conventional QCD processes [198, 222, 223, 224, 225, 226, 227, 228, 219, 229, 230, 202, 231, 232, 233, 234]. For example, the N-subjettiness algorithm [235] aims to determine the consistency of a jet with a hypothesized number of subjets. Such tools can give good discrimination between top quark jets and QCD jets, however, such discrimination degrades somewhat with the additional pileup activity.

It is also beneficial to identify the two subjets corresponding to the W boson produced in the top quark decay. Using trimming, a W mass peak can be extracted which is relatively stable even with 140 additional pileup events added.

Top tagging. In addition to the substructure quantities described above, there are several algorithms (top taggers) which combine multiple jet observables to identify top jets and provide additional discrimination from QCD jets. Two top-tagging algorithms which are currently in use by experimental efforts include the CMS Top Tagger [230, 226] and the HEP Top Tagger [156, 236, 237, 238, 196]. The CMS top tagger decomposes a jet into up to 4 subjets. Then requirements on the jet mass ($140 < m_j < 250$ GeV), number of subjets (3 or more) and a quantity which is a proxy for the mass of the W boson within the jet (minimum pairwise subjet mass > 50 GeV) , are imposed to isolate boosted top quarks. We have studied the effect of pileup on the efficiency of the CMS top tagger. With no additional pileup events, the efficiency of the algorithm maintains its maximum value of $\sim 40\%$ up to jet p_T values of 1.2-1.3 TeV, at which point the efficiency begins to fall to 10% or lower for jets with $p_T > 1.5$ TeV. This efficiency drop at high p_T can

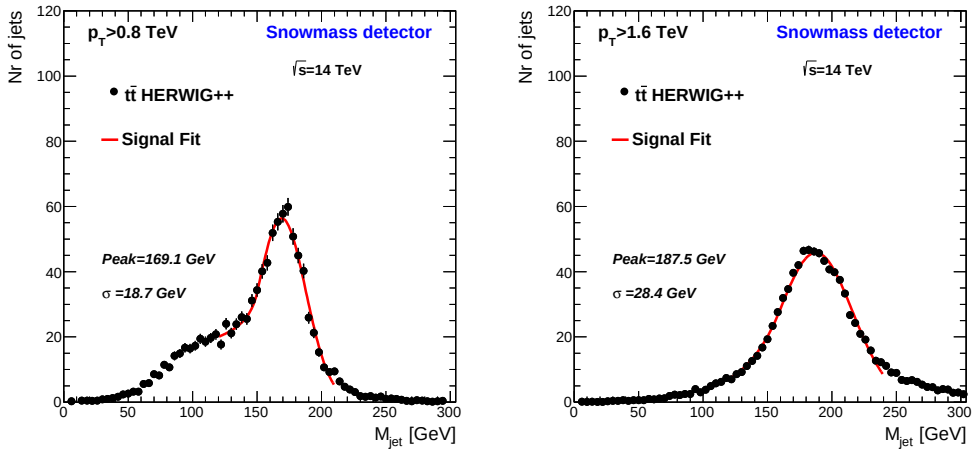

(a) $p_T(jet) > 0.8$ TeV (b) $p_T(jet) > 1.6$ TeV

Figure 1-7. *Jet mass for $t\bar{t}$ events for different p_T(jet) and $\langle\mu\rangle = 140$. The core of the peak was fitted using a Crystal Ball function [239]. All histograms are normalized to 1000 events.*

be ameliorated by increasing calorimeter granularity, but extra radiation off of the top quark also affects the algorithm in the very high p_T regime. With additional pileup events (and no correction applied to the subjets), the efficiency degradation happens at much lower p_T values. The rate of QCD jets passing the algorithm is also affected. With no additional pileup events, this mistag rate remains below 5% over the entire range of jet p_T. After adding 140 pileup interactions to the simulated events, the mistag rate from QCD jets increases to a maximum of 45% at a p_T of 500 GeV, though this can be reduced through additional algorithm improvements. However, above approximately $p_T > 1$ TeV we expect that there will be minimal impact after pile-up corrections.

Detector effects. At large values of the top quark p_T, such as the region above 1.5 TeV at the LHC, QCD radiation as well as the size of the detector elements become a limiting factor. In this regime, top quarks will have hard radiations that may be identified as subjets and the top quark decay products become so highly collimated that they cannot be individually resolved due to calorimeter detector segmentation and tracking failures.

The effects mentioned above cause a degradation in the top quark jet resolution at large p_T. For example, the width of the top quark jet mass peak increases by a factor of two when comparing top quarks with $p_T > 1.6$ TeV to those with $p_T > 0.8$ TeV, see Fig. 1-7. Algorithmic improvements extend the p_T range where top jets can be reconstructed, but ultimately the granularity of individual calorimeter cells must be increased to maintain a good top jet reconstruction.

The reconstruction of top jets and substructure within large cone-size jets is a relatively new field that has made tremendous progress in only a few years. More improvements are likely to come, especially as sizable top quark event samples at the highest momenta become available at the LHC. The ultimate limit is expected to come from the detector resolution, particularly from calorimeter granularity, and future detectors such as for CLIC or VLHC machines will need account for this.

1.7.3 Lepton colliders

A lepton collider (linear e^+e^- colliders ILC and CLIC and circular e^+e^- collider TLEP and the $\mu^+\mu^-$ collider) will allow for the study of electroweak production of $t\bar{t}$ pairs with no concurring QCD background. Linear colliders can use polarized beams, giving samples enriched in top quarks of left- or right-handed helicities. This can allow one to probe new physics scenarios predicting anomalous production rates of right-handed t quarks compared to the SM, and to disentangle the $t\gamma$ and tZ couplings, see Section 1.3.

Due to the electroweak production mechanism, all interesting processes occur at roughly the same rate, and backgrounds can easily be reduced to a negligible level. After applying selection cuts, it is possible to retain a signal sample of approximately 10^5 events at the 500 GeV linear collider with 500 fb^{-1} of integrated luminosity. Unlike at the LHC, there are no or few additional interactions (pileup) per beam crossing, especially for the ILC. Additional activity may come from $\gamma\gamma$ interactions. Ongoing studies show that this residual pile-up can be controlled when applying the invariant k_t jet algorithm [240, 241] for background suppression [242].

The lepton collider detectors can be designed to be more fine-grained and to have better resolution than the LHC detectors. The charge of the b quark will be measured at a purity of 60% and better [116]. This is indispensable for the measurement of A_{FB}^t in fully hadronic decays, see Section 1.4. The jet energy resolution for LHC detectors is between 10% and 15% for jets below 100 GeV [243] whereas it is below 4% at the linear collider [22]. This results in a clean top quark sample with a narrow reconstructed mass as shown in Fig. 1-1.

Using A_{FB}^t, the top-Higgs coupling λ_t and the $t\bar{t}$ production cross-section, electroweak couplings can be determined at the percent level. It is important that experimental and theoretical errors are kept at the same level. This requires a precise measurement of the luminosity and the beam polarization. Currently, both parameters are expected to be controlled to better than 0.5% at the linear collider. In general the realization of machine and detectors must not compromise the precision physics. This may be the biggest challenge in the coming years.

1.8 Conclusions

This is the concluding section for top quark snowmass 2013 studies. We have discussed six topics – the top quark mass, top quark couplings to other SM particles, kinematics of top-like final states, rare decays of top quarks and top quark physics beyond the Standard Model. We will describe our conclusions for each of these topics.

We have argued that a theoretically clean measurement of the top mass to about 300 MeV is sufficient for many of the physics goals that are currently discussed, in particular electroweak precision fits. If no new physics is found at the LHC, it will be important to address the vacuum stability issue of the SM. To address this, a top mass measurement with a precision of 100 MeV is required, given the expected precision of the Higgs mass measurement. The top quark mass can be measured with an accuracy of about 500 MeV in individual measurements at the LHC, and their combination might reduce the uncertainty further. We note that both novel methods and the high-luminosity option are required for achieving this accuracy. The top mass can be measured with an accuracy of about 100 MeV (dominated by theoretical uncertainties) at a lepton collider, which matches well with the precision on the W mass achievable at such a facility.

While the LHC and a future linear collider provide complementary information on top quark couplings, there is no doubt that the LHC, especially the high-luminosity option, will probe a majority of top quark couplings to gluons, photons, Z's, W's and the Higgs boson with precision that should allow us to detect deviations

caused by generic BSM physics at the TeV scale. The much higher precision achievable at a linear collider should then either allow us to study these deviations or exclude the existence of generic BSM physics at even higher scales, in particular for the γ and Z couplings. The top Yukawa coupling, one of the most important top couplings, will be measured to roughly equal precision at the LHC and the 500 GeV ILC and to better precision at a high-energy linear collider.

Understanding how top quarks are produced and decay is an integral part of top physics at any collider. Kinematic distributions and differential cross sections are the key to achieving this goal. The measurement of basic top observables will help improve modeling of top quark events. The large top event samples available in the future will allow the study of new observables such as angular correlations or asymmetries that can uncover subtle new physics effects which may not be accessible otherwise. We expect the LHC may be able to resolve the Tevatron A_{FB} discrepancy.

The LHC and a future linear collider are complementary in probing rare decays of the top quark. The LHC is better at probing flavor-changing couplings involving gluons, with about a factor two improvement in the branching ratio limits expected from the high-luminosity option. A linear collider is better for processes involving γ's and Z's. If rare decays are found, a linear collider also is able to probe the spin structure of the couplings involved.

Top quarks play a very important role in searches for physics beyond the SM. In particular, solutions to the hierarchy problem require new particles decaying to top-like final states, such as stops in SUSY or top partners in other models. The LHC is able to cover the region of interest up to a few TeV in mass for stops, top-partners and resonances decaying into top quarks. The high-luminosity option extends the mass reach for these particles by roughly 50%. Given the current limits, only a multi-TeV lepton collider will be able to produce top partners and resonances directly. We note that there are stop models that might be difficult to discover at the LHC but can be probed at a linear collider, for example stealth stops.

The 14 TeV LHC is a complex environment, especially the high pileup of the high-luminosity option which makes precision measurements of top mass, couplings and kinematic distributions challenging. Moreover, the 14 TeV LHC provides a large sample of boosted top quarks for the first time whose decay products can no longer be individually identified using traditional techniques. Our studies indicate that both of these challenges can be mitigated with algorithm developments and other improvements, many of which have not been deployed yet for these Snowmass studies in the high-luminosity scenario. In particular, many analyses will need to rely on these algorithms in future data collection periods, to maintain sensitivity to new physics processes in the high-mass regime The experimental environment at a lepton collider does not suffer from these problems and instead offers an ideal environment for precision top physics; there are few or no additional interactions per crossing and the detectors are more fine-grained and have better resolution.

In summary, the LHC and the HL-LHC will in two stages dramatically improve our knowledge of the top quark and extends the reach for new physics to interesting and relevant regions. A future lepton collider will be able to study the top quark in even more detail, in particular its mass and couplings. We are confident that the predictions in this report are conservative and that the experiments will do better with actual data than predicted here.

References

[1] CDF Collaboration. Observation of top quark production in $\bar{p}p$ collisions. *Phys.Rev.Lett.*, 74:2626–2631, 1995, hep-ex/9503002.

[2] D0 Collaboration. Observation of the top quark. *Phys.Rev.Lett.*, 74:2632–2637, 1995, hep-ex/9503003.

[3] Giuseppe Degrassi, Stefano Di Vita, Joan Elias-Miro, Jose R. Espinosa, Gian F. Giudice, et al. Higgs mass and vacuum stability in the Standard Model at NNLO. *JHEP*, 1208:098, 2012, 1205.6497.

[4] M. Baak, A. Blondel, A. Bodek, R. Caputo, T. Corbett, et al. Study of Electroweak Interactions at the Energy Frontier. 2013, 1310.6708.

[5] M. Baak, M. Goebel, J. Haller, A. Hoecker, D. Kennedy, et al. The Electroweak Fit of the Standard Model after the Discovery of a New Boson at the LHC. *Eur.Phys.J.*, C72:2205, 2012, 1209.2716.

[6] P. Janot, M. M. Bachtis, and A. Blondel. First Look at the Physics Case of TLEP. 2013, arXiv:1308.6176, SNOW13-00127.

[7] Katja Seidel, Frank Simon, Michal Tesar, and Stephane Poss. Top quark mass measurements at and above threshold at CLIC. 2013, 1303.3758.

[8] Manel Martinez and Ramon Miquel. Multiparameter fits to the t anti-t threshold observables at a future e+ e- linear collider. *Eur.Phys.J.*, C27:49–55, 2003, hep-ph/0207315.

[9] D. Asner, A. Hoang, Y. Kiyo, R. Pschl, Y. Sumino, et al. Top quark precision physics at the International Linear Collider. 2013, 1307.8265.

[10] Martin Beneke, Yuichiro Kiyo, and Kurt Schuller. NNNLO results on top-quark pair production near threshold. *PoS*, RADCOR2007:051, 2007, 0801.3464.

[11] James S. Gainer, Joseph Lykken, Konstantin T. Matchev, Stephen Mrenna, and Myeonghun Park. The Matrix Element Method: Past, Present, and Future. 2013, 1307.3546.

[12] ATLAS Collaboration. Measurement of the top quark mass with the template method in the $t\bar{t}$ lepton + jets channel using ATLAS data. *Eur.Phys.J.*, C72:2046, 2012, 1203.5755.

[13] CMS Collaboration. Measurement of the top-quark mass in $t\bar{t}$ events with lepton+jets final states in pp collisions at $\sqrt{s} = 7$ TeV. *JHEP*, 1212:105, 2012, 1209.2319.

[14] CMS Collaboration. Measurement of masses in the $t\bar{t}$ system by kinematic endpoints in pp collisions at $\sqrt{s} = 7$ TeV. 2013, 1304.5783.

[15] Avto Kharchilava. Top mass determination in leptonic final states with J/ψ. *Phys.Lett.*, B476:73–78, 2000, hep-ph/9912320.

[16] Ansgar Denner, Stefan Dittmaier, Stefan Kallweit, and Stefano Pozzorini. NLO QCD corrections to off-shell top-antitop production with leptonic decays at hadron colliders. *JHEP*, 1210:110, 2012, 1207.5018.

[17] Giuseppe Bevilacqua, Michal Czakon, Andreas van Hameren, Costas G. Papadopoulos, and Malgorzata Worek. Complete off-shell effects in top quark pair hadroproduction with leptonic decay at next-to-leading order. *JHEP*, 1102:083, 2011, 1012.4230.

[18] ATLAS Collaboration. Measurement of the Top Quark Mass from $\sqrt{s} = 7$ TeV ATLAS data using a 3-dimensional template fit. *ATLAS-CONF-2013-046*, 2013.

[19] Sandip Biswas, Kirill Melnikov, and Markus Schulze. Next-to-leading order QCD effects and the top quark mass measurements at the LHC. *JHEP*, 1008:048, 2010, 1006.0910.

[20] Simone Alioli, Patricia Fernandez, Juan Fuster, Adrian Irles, Sven-Olaf Moch, et al. A new observable to measure the top-quark mass at hadron colliders. *Eur.Phys.J.*, C73:2438, 2013, 1303.6415.

[21] D0 Collaboration. An Improved determination of the width of the top quark. *Phys.Rev.*, D85:091104, 2012, 1201.4156.

[22] Howard Baer, Tim Barklow, Keisuke Fujii, Yuanning Gao, Andre Hoang, et al. The International Linear Collider Technical Design Report - Volume 2: Physics. 2013, 1306.6352.

[23] A. Juste, Y. Kiyo, F. Petriello, T. Teubner, K. Agashe, et al. Report of the 2005 Snowmass top/QCD working group. 2006, hep-ph/0601112.

[24] J.A. Aguilar-Saavedra. A Minimal set of top anomalous couplings. *Nucl.Phys.*, B812:181–204, 2009, 0811.3842.

[25] Cen Zhang and Scott Willenbrock. Effective Field Theory for Top Quark Physics. *Nuovo Cim.*, C033N4:285–291, 2010, 1008.3155.

[26] Michal Czakon, Paul Fiedler, and Alexander Mitov. The total top quark pair production cross-section at hadron colliders through $O(alpha_S^4)$. 2013, 1303.6254.

[27] Peter Baernreuther, Michal Czakon, and Alexander Mitov. Percent Level Precision Physics at the Tevatron: First Genuine NNLO QCD Corrections to $q\bar{q} \to t\bar{t} + X$. *Phys.Rev.Lett.*, 109:132001, 2012, 1204.5201.

[28] Michal Czakon and Alexander Mitov. NNLO corrections to top-pair production at hadron colliders: the all-fermionic scattering channels. *JHEP*, 1212:054, 2012, 1207.0236.

[29] J.H. Khn, A. Scharf, and P. Uwer. Weak Interactions in Top-Quark Pair Production at Hadron Colliders: An Update. 2013, 1305.5773.

[30] Matthew Baumgart and Brock Tweedie. A New Twist on Top Quark Spin Correlations. *JHEP*, 1303:117, 2013, 1212.4888.

[31] J Adelman, M Baumgart, A Garcia-Bellido, and A Loginov. Determining Top Quark Couplings at the LHC: Snowmass White Paper. 2013, arXiv:1308.5274, SNOW13-00154.

[32] ATLAS Collaboration. Measurement of the top quark pair production cross section in the single-lepton channel with ATLAS in proton-proton collisions at 8 TeV using kinematic fits with b-tagging. Technical Report ATLAS-CONF-2012-149, CERN, Geneva, Nov 2012.

[33] ATLAS and CMS Collaborations. Combination of ATLAS and CMS top-quark pair cross section measurements using up to 1.1 fb^{-1} of data at 7 TeV. Technical Report ATLAS-CONF-2012-134, CMS-PAS-TOP-12-003, CERN, Geneva, Sep 2012.

[34] CMS Collaboration. Top pair cross section in dileptons. Technical Report CMS-PAS-TOP-12-007, CERN, Geneva, 2012.

[35] Nikolaos Kidonakis. NNLL threshold resummation for top-pair and single-top production. 2012, 1210.7813.

[36] ATLAS Collaboration. Measurement of the t-channel single top-quark production cross section in pp collisions at $\sqrt{s} = 7$ TeV with the ATLAS detector. *Phys.Lett.*, B717:330–350, 2012, 1205.3130.

[37] ATLAS Collaboration. Measurement of t-channel Single Top-Quark Production in pp Collisions at $\sqrt{s} = 8$ TeV with the ATLAS detector. Technical Report ATLAS-CONF-2012-132, CERN, Geneva, Sep 2012.

[38] CMS Collaboration. Measurement of the single-top-quark t-channel cross section in pp collisions at $\sqrt{s} = 7$ TeV. *JHEP*, 1212:035, 2012, 1209.4533.

[39] CMS Collaboration. Measurement of the single-top t-channel cross section in pp collisions at centre-of-mass energy of 8 TeV. Technical Report CMS-PAS-TOP-12-011, CERN, Geneva, 2012.

[40] ATLAS Collaboration. Evidence for the associated production of a W boson and a top quark in ATLAS at $\sqrt{s} = 7$ TeV. *Phys.Lett.*, B716:142–159, 2012, 1205.5764.

[41] ATLAS Collaboration. Measurement of the cross-section for associated production of a top quark and a W boson at $\sqrt{s} = 8$ TeV with the ATLAS detector. Technical Report ATLAS-CONF-2013-100, CERN, Geneva, 2013.

[42] CMS Collaboration. Evidence for associated production of a single top quark and W boson in pp collisions at 7 TeV. *Phys.Rev.Lett.*, 2012, 1209.3489.

[43] CMS Collaboration. Observation of associated production of a single top quark and w boson in pp collisions at sqrt(s) = 8 tev. Technical Report CMS-PAS-TOP-12-040, CERN, Geneva, 2013.

[44] Nicola Cabibbo. Unitary Symmetry and Leptonic Decays. *Phys.Rev.Lett.*, 10:531–533, 1963.

[45] Andrzej Czarnecki, Jurgen G. Korner, and Jan H. Piclum. Helicity fractions of W bosons from top quark decays at NNLO in QCD. *Phys.Rev.*, D81:111503, 2010, 1005.2625.

[46] Jun Gao, Chong Sheng Li, and Hua Xing Zhu. Top Quark Decay at Next-to-Next-to Leading Order in QCD. *Phys.Rev.Lett.*, 110:042001, 2013, 1210.2808.

[47] Mathias Brucherseifer, Fabrizio Caola, and Kirill Melnikov. $\mathcal{O}(\alpha_s^2)$ corrections to fully-differential top quark decays. *JHEP*, 1304:059, 2013, 1301.7133.

[48] H. Lacker, A. Menzel, F. Spettel, D. Hirschbuhl, J. Luck, et al. Model-independent extraction of $|V_{tq}|$ matrix elements from top-quark measurements at hadron colliders. *Eur.Phys.J.*, C72:2048, 2012, 1202.4694.

[49] Brad Schoenrock, Elizabeth Drueke, Barbara Alvarez Gonzalez, and Reinhard Schwienhorst. Single top quark cross section measurement in the t-channel at the high-luminosity LHC. 2013, arXiv:1308.6307 and SNOW13-00156.

[50] ATLAS Collaboration. Search for $\mathcal{CP}$ violation in single top quark events in pp collisions at $\sqrt{s} = 7$ tev with the atlas detector. Technical Report ATLAS-CONF-2013-032, CERN, Geneva, 2013.

[51] E. Boos, M. Dubinin, A. Pukhov, M. Sachwitz, and H.J. Schreiber. Single top production in e+ e-, e- e-, gamma e and gamma gamma collisions. *Eur.Phys.J.*, C21:81–91, 2001, hep-ph/0104279.

[52] Sukanta Dutta, Ashok Goyal, Mukesh Kumar, and Bruce Mellado. Measuring anomalous Wtb couplings at $e^- p$ collider. 2013, 1307.1688.

[53] ATLAS Collaboration. Measurement of the top quark charge in pp collisions at sqrt(s) = 7 TeV with the ATLAS detector. 2013, 1307.4568.

[54] ATLAS Collaboration. Measurement of the inclusive t tbar gamma cross section with the atlas detector. Technical Report ATLAS-CONF-2011-153, CERN, Geneva, Nov 2011.

[55] U. Baur, A. Juste, D. Rainwater, and L.H. Orr. Improved measurement of ttZ couplings at the CERN LHC. *Phys.Rev.*, D73:034016, 2006, hep-ph/0512262.

[56] U. Baur, A. Juste, L.H. Orr, and D. Rainwater. Probing electroweak top quark couplings at hadron colliders. *Phys.Rev.*, D71:054013, 2005, hep-ph/0412021.

[57] Achilleas Lazopoulos, Thomas McElmurry, Kirill Melnikov, and Frank Petriello. Next-to-leading order QCD corrections to $t\bar{t}Z$ production at the LHC. *Phys.Lett.*, B666:62–65, 2008, 0804.2220.

[58] Kirill Melnikov, Markus Schulze, and Andreas Scharf. QCD corrections to top quark pair production in association with a photon at hadron colliders. *Phys.Rev.*, D83:074013, 2011, 1102.1967.

[59] M.V. Garzelli, A. Kardos, C.G. Papadopoulos, and Z. Trocsanyi. t $\bar{t}$ W^{+-} and t $\bar{t}$ Z Hadroproduction at NLO accuracy in QCD with Parton Shower and Hadronization effects. *JHEP*, 1211:056, 2012, 1208.2665.

[60] M.V. Garzelli, A. Kardos, C.G. Papadopoulos, and Z. Trocsanyi. Z0 - boson production in association with a top anti-top pair at NLO accuracy with parton shower effects. *Phys.Rev.*, D85:074022, 2012, 1111.1444.

[61] John Campbell, R. Keith Ellis, and Raoul Rntsch. Single top production in association with a Z boson at the LHC. 2013, 1302.3856.

[62] J. Adelman, B. Alvarez Gonzalez, Y. Bai, M. Baumgart, R. K. Ellis, A Khanov, A Loginov, and M. Vos. Top Couplings: pre-Snowmass Energy Frontier 2013 Overview. 2013, arXiv:1309.1947, SNOW13-00155.

[63] S. Dawson, A. Gritsan, H. Logan, J. Qian, C. Tully, et al. Higgs Working Group Report of the Snowmass 2013 Community Planning Study. 2013, arXiv:1310.8361.

[64] Christopher Boddy, Sinead Farrington, and Christopher Hays. Higgs boson coupling sensitivity at the lhc using $h \to \tau\tau$ decays. *Phys. Rev. D*, 86:073009, Oct 2012.

[65] Peter Onyisi, Robert Kehoe, Victor Rodriguez, and Yuriy Ilchenko. Analysis of t tbar H Events at sqrt(s)=14 TeV with H to WW. 2013, 1307.7280.

[66] CMS Collaboration. Cms at the high-energy frontier. contribution to the update of the european strategy for particle physics. Technical Report CMS-NOTE-2012-006. CERN-CMS-NOTE-2012-006, CERN, Geneva, Oct 2012.

[67] ATLAS Collaboration. Physics at a high-luminosity lhc with atlas (update). Technical Report ATL-PHYS-PUB-2012-004, CERN, Geneva, Oct 2012.

[68] Jared Vasquez, Jahred Adelman, Andrey Loginov, and Paul Tipton. Study of ttH ($H \to \mu\mu$) in the three lepton channel at sqrt(s) = 14 TeV; A Snowmass white paper. 2013, 1310.1132.

[69] J. Gunion and X.-G. He. *Phys. Rev. Lett.*, 76:4468–4471, 1996, hep-ph/9602226.

[70] Ryo Yonamine, Katsumasa Ikematsu, Tomohiko Tanabe, Keisuke Fujii, Yuichiro Kiyo, et al. Measuring the top Yukawa coupling at the ILC at $\sqrt{s} = 500$ GeV. *Phys.Rev.*, D84:014033, 2011, 1104.5132.

[71] CLIC Detector and Physics Study Collaboration. Physics at the CLIC e+e- Linear Collider – Input to the Snowmass process 2013. 2013, 1307.5288.

[72] Kirill Melnikov and Markus Schulze. NLO QCD corrections to top quark pair production and decay at hadron colliders. *JHEP*, 0908:049, 2009, 0907.3090.

[73] John M. Campbell and R. Keith Ellis. Top-quark processes at NLO in production and decay. 2012, 1204.1513.

[74] Kirill Melnikov and Markus Schulze. NLO QCD corrections to top quark pair production in association with one hard jet at hadron colliders. *Nucl.Phys.*, B840:129–159, 2010, 1004.3284.

[75] S. Dittmaier, P. Uwer, and S. Weinzierl. Hadronic top-quark pair production in association with a hard jet at next-to-leading order QCD: Phenomenological studies for the Tevatron and the LHC. *Eur. Phys. J.*, C59:625–646, 2009, 0810.0452.

[76] Adam Kardos, Costas Papadopoulos, and Zoltan Trocsanyi. Top quark pair production in association with a jet with NLO parton showering. *Phys.Lett.*, B705:76–81, 2011, 1101.2672.

[77] John M. Campbell and R.K. Ellis. MCFM for the Tevatron and the LHC. *Nucl.Phys.Proc.Suppl.*, 205-206:10–15, 2010, 1007.3492.

[78] Andreas Jung, Markus Schulze, and Jessie Shelton. Kinematics of Top Quark Final States: A Snowmass White Paper. 2013, arXiv:1309.2889, SNOW13-00153.

[79] Valentin Ahrens, Andrea Ferroglia, Matthias Neubert, Ben D. Pecjak, and Li-Lin Yang. RG-improved single-particle inclusive cross sections and forward-backward asymmetry in $t\bar{t}$ production at hadron colliders. *JHEP*, 1109:070, 2011, 1103.0550.

[80] B. Auerbach, S.V. Chekanov, and N. Kidonakis. Studies of highly-boosted top quarks near the TeV scale using jet masses at the LHC. 2013, 1301.5810. arXiv:1301.5810, SNOW13-00027.

[81] D0 Collaboration. Evidence for spin correlation in $t\bar{t}$ production. *Phys.Rev.Lett.*, 108:032004, 2012, 1110.4194.

[82] ATLAS Collaboration. Observation of spin correlation in $t\bar{t}$ events from pp collisions at sqrt(s) = 7 TeV using the ATLAS detector. *Phys.Rev.Lett.*, 108:212001, 2012, 1203.4081.

[83] CMS Collaboration. Measurement of spin correlations in ttbar production. Technical Report CMS-PAS-TOP-12-004, CERN, Geneva, 2012.

[84] Gregory Mahlon and Stephen J. Parke. Spin Correlation Effects in Top Quark Pair Production at the LHC. *Phys.Rev.*, D81:074024, 2010, 1001.3422.

[85] Werner Bernreuther and Zong-Guo Si. Distributions and correlations for top quark pair production and decay at the Tevatron and LHC. *Nucl.Phys.*, B837:90–121, 2010, 1003.3926.

[86] Stefano Frixione, Eric Laenen, Patrick Motylinski, and Bryan R. Webber. Angular correlations of lepton pairs from vector boson and top quark decays in Monte Carlo simulations. *JHEP*, 0704:081, 2007, hep-ph/0702198.

[87] Zhenyu Han, Andrey Katz, David Krohn, and Matthew Reece. (Light) Stop Signs. *JHEP*, 1208:083, 2012, 1205.5808.

[88] Werner Bernreuther and Zong-Guo Si. Top quark spin correlations and polarization at the LHC: standard model predictions and effects of anomalous top chromo moments. 2013, 1305.2066.

[89] Matthew Baumgart and Brock Tweedie. Discriminating Top-Antitop Resonances using Azimuthal Decay Correlations. *JHEP*, 1109:049, 2011, 1104.2043.

[90] Fabrizio Caola, Kirill Melnikov, and Markus Schulze. A complete next-to-leading order QCD description of resonant Z' production and decay into $t\bar{t}$ final states. *Phys.Rev.*, D87:034015, 2013, 1211.6387.

[91] Johann H. Kuhn and German Rodrigo. Charge asymmetry in hadroproduction of heavy quarks. *Phys.Rev.Lett.*, 81:49–52, 1998, hep-ph/9802268.

[92] Johann H. Kuhn and German Rodrigo. Charge asymmetry of heavy quarks at hadron colliders. *Phys.Rev.*, D59:054017, 1999, hep-ph/9807420.

[93] Leandro G. Almeida, George Sterman, and Werner Vogelsang. Threshold resummation for the top quark charge asymmetry. *Phys. Rev. D*, 78:014008, Jul 2008.

[94] Oscar Antuñano, Johann H. Kühn, and Germán Rodrigo. Top quarks, axigluons, and charge asymmetries at hadron colliders. *Phys. Rev. D*, 77:014003, Jan 2008.

[95] M. T. Bowen, S. D. Ellis, and D. Rainwater. Standard model top quark asymmetry at the fermilab tevatron. *Phys. Rev. D*, 73:014008, Jan 2006.

[96] CDF Collaboration. Measurement of the top quark forward-backward production asymmetry and its dependence on event kinematic properties. *Phys. Rev. D*, 87:092002, May 2013.

[97] D0 Collaboration. Measurement of leptonic asymmetries and top-quark polarization in $t\bar{t}$ production. *Phys. Rev. D*, 87:011103, Jan 2013.

[98] ATLAS Collaboration. Measurement of the charge asymmetry in top quark pair production in pp collisions at $\sqrt{s} = 7$ TeV using the ATLAS detector. *Eur.Phys.J.*, C72:2039, 2012, 1203.4211.

[99] CMS Collaboration. Measurement of the charge asymmetry in top-quark pair production in proton-proton collisions at. *Physics Letters B*, 709(12):28 – 49, 2012.

[100] Werner Bernreuther and Zong-Guo Si. Top quark and leptonic charge asymmetries for the tevatron and lhc. *Phys. Rev. D*, 86:034026, Aug 2012.

[101] ATLAS Collaboration. Measurement of the charge asymmetry in dileptonic decay of top quark pairs in pp collisions at $\sqrt{s} = 7$ TeV using the ATLAS detector. Technical Report ATLAS-CONF-2012-057, CERN, Geneva, Jun 2012.

[102] CMS Collaboration. Top charge asymmetry measurement in dileptons at 7 TeV. Technical Report CMS-PAS-TOP-12-010, CERN, Geneva, 2012.

[103] R Gauld, on behalf of the LHCb Collaboration. Measuring top quark production asymmetries at lhcb. *LHCb-PUB-2013-009*, 2013.

[104] Alexander L. Kagan, Jernej F. Kamenik, Gilad Perez, and Sheldon Stone. Top LHCb Physics. *Phys.Rev.Lett.*, 107:082003, 2011, 1103.3747.

[105] Paul H. Frampton, Jing Shu, and Kai Wang. Axigluon as Possible Explanation for p anti-p -¿ t anti-t Forward-Backward Asymmetry. *Phys.Lett.*, B683:294–297, 2010, 0911.2955.

[106] Yang Bai, JoAnne L. Hewett, Jared Kaplan, and Thomas G. Rizzo. LHC Predictions from a Tevatron Anomaly in the Top Quark Forward-Backward Asymmetry. *JHEP*, 1103:003, 2011, 1101.5203.

[107] Gustavo Marques Tavares and Martin Schmaltz. Explaining the t-tbar asymmetry with a light axigluon. *Phys.Rev.*, D84:054008, 2011, 1107.0978.

[108] Moira Gresham, Jessie Shelton, and Kathryn M. Zurek. Open windows for a light axigluon explanation of the top forward-backward asymmetry. *JHEP*, 1303:008, 2013, 1212.1718.

[109] Ulrich Haisch and Susanne Westhoff. Massive Color-Octet Bosons: Bounds on Effects in Top-Quark Pair Production. *JHEP*, 1108:088, 2011, 1106.0529.

[110] Stefan Berge and Susanne Westhoff. Top-Quark Charge Asymmetry Goes Forward: Two New Observables for Hadron Colliders. 2013, 1305.3272.

[111] Stefan Berge and Susanne Westhoff. Charge Asymmetry in Top Pair plus Jet Production. 2013, 1307.6225.

[112] Edmond L. Berger, Qing-Hong Cao, Chuan-Ren Chen, Jiang-Hao Yu, and Hao Zhang. The Top Quark Production Asymmetries A_{FB}^t and A_{FB}^ℓ. *Phys.Rev.Lett.*, 108:072002, 2012, 1201.1790.

[113] M.S. Amjad et al. A precise determination of top quark electroweak couplings at the ILC operating at $\sqrt{s} = 500\,\text{GeV}$. *LC-REP-2013-007*, 2013.

[114] Wolfgang Kilian, Thorsten Ohl, and Jurgen Reuter. WHIZARD: Simulating Multi-Particle Processes at LHC and ILC. *Eur.Phys.J.*, C71:1742, 2011, 0708.4233.

[115] Mauro Moretti, Thorsten Ohl, and Jurgen Reuter. O'Mega: An Optimizing matrix element generator. *IKDA-2001-06, LC-TOOL-2001-040, hep-ph/0102195*, 2001, hep-ph/0102195.

[116] Erik Devetak, Andrei Nomerotski, and Michael Peskin. Top quark anomalous couplings at the International Linear Collider. *Phys.Rev.*, D84:034029, 2011, 1005.1756.

[117] A.H. Hoang, M. Beneke, K. Melnikov, T. Nagano, A. Ota, et al. Top - anti-top pair production close to threshold: Synopsis of recent NNLO results. *Eur.Phys.J.direct*, C2:1, 2000, hep-ph/0001286.

[118] N. Craig and M. Velasco. Top Rare Decays. *Snowmass whitepaper, in preparation*, 2013.

[119] J.A. Aguilar-Saavedra. Top flavor-changing neutral interactions: Theoretical expectations and experimental detection. *Acta Phys.Polon.*, B35:2695–2710, 2004, hep-ph/0409342.

[120] David Atwood, Laura Reina, and Amarjit Soni. Phenomenology of two Higgs doublet models with flavor changing neutral currents. *Phys.Rev.*, D55:3156–3176, 1997, hep-ph/9609279.

[121] Santi Bejar. Flavor changing neutral decay effects in models with two Higgs boson doublets: Applications to LHC Physics. 2006, hep-ph/0606138.

[122] J.J. Cao, G. Eilam, M. Frank, K. Hikasa, G.L. Liu, et al. SUSY-induced FCNC top-quark processes at the large hadron collider. *Phys.Rev.*, D75:075021, 2007, hep-ph/0702264.

[123] Jin Min Yang, Bing-Lin Young, and X. Zhang. Flavor changing top quark decays in r parity violating SUSY. *Phys.Rev.*, D58:055001, 1998, hep-ph/9705341.

[124] G. Eilam, A. Gemintern, Tao Han, J.M. Yang, and X. Zhang. Top quark rare decay $t \to ch$ in R-parity violating SUSY. *Phys.Lett.*, B510:227–235, 2001, hep-ph/0102037.

[125] Kaustubh Agashe, Gilad Perez, and Amarjit Soni. Collider Signals of Top Quark Flavor Violation from a Warped Extra Dimension. *Phys.Rev.*, D75:015002, 2007, hep-ph/0606293.

[126] Kaustubh Agashe and Roberto Contino. Composite Higgs-Mediated FCNC. *Phys.Rev.*, D80:075016, 2009, 0906.1542.

[127] G. Eilam, J.L. Hewett, and A. Soni. Rare decays of the top quark in the standard and two Higgs doublet models. *Phys.Rev.*, D44:1473–1484, 1991.

[128] B. Mele, S. Petrarca, and A. Soddu. A New evaluation of the $t \to cH$ decay width in the standard model. *Phys.Lett.*, B435:401–406, 1998, hep-ph/9805498.

[129] Michael E. Luke and Martin J. Savage. Flavor changing neutral currents in the Higgs sector and rare top decays. *Phys.Lett.*, B307:387–393, 1993, hep-ph/9303249.

[130] CMS Collaboration. Search for flavor changing neutral currents in top quark decays in pp collisions at 7 TeV. *Phys.Lett.*, B718:1252–1272, 2013, 1208.0957.

[131] The ATLAS collaboration. Search for single top-quark production via FCNC in strong interaction in $\sqrt{s} = 8$ TeV ATLAS data. 2013.

[132] CDF Collaboration. Search for flavor-changing neutral current decays of the top quark in $p\bar{p}$ collisions at $\sqrt{s} = 1.8$ TeV. *Phys.Rev.Lett.*, 80:2525–2530, 1998.

[133] CDF Collaboration. Search for Invisible Top Decays with 1.9 fb-1 of CDF-II Data. *CDF/PUB/TOP/PUBLIC/9496*, 2008.

[134] H1 Collaboration. Search for Single Top Quark Production at HERA. *Phys.Lett.*, B678:450–458, 2009, 0904.3876.

[135] The ATLAS collaboration. Search for flavor-changing neutral currents in $t \to cH$, with $H \to \gamma\gamma$, and limit on the tcH coupling. 2013.

[136] Nathaniel Craig, Jared A. Evans, Richard Gray, Michael Park, Sunil Somalwar, et al. Searching for $t \to ch$ with Multi-Leptons. *Phys.Rev.*, D86:075002, 2012, 1207.6794.

[137] ATLAS Collaboration. A search for flavour changing neutral currents in top-quark decays in pp collision data collected with the ATLAS detector at $\sqrt{s} = 7$ TeV. *JHEP*, 1209:139, 2012, 1206.0257.

[138] Patrick J. Fox, Zoltan Ligeti, Michele Papucci, Gilad Perez, and Matthew D. Schwartz. Deciphering top flavor violation at the LHC with B factories. *Phys.Rev.*, D78:054008, 2008, 0704.1482.

[139] Roni Harnik, Joachim Kopp, and Jure Zupan. Flavor Violating Higgs Decays. *JHEP*, 1303:026, 2013, 1209.1397.

[140] ATLAS Collaboration. Physics at a High-Luminosity LHC with ATLAS. 2013, 1307.7292.

[141] J.A. Aguilar-Saavedra and T. Riemann. Probing top flavor changing neutral couplings at TESLA. 2001, hep-ph/0102197.

[142] Jun Gao, Chong Sheng Li, Li Lin Yang, and Hao Zhang. Search for anomalous top quark production at the early LHC. *Phys.Rev.Lett.*, 107:092002, 2011, 1104.4945.

[143] ATLAS Collaboration. Search for FCNC single top-quark production at $\sqrt{s} = 7$ TeV with the ATLAS detector. *Phys.Lett.*, B712:351–369, 2012, 1203.0529.

[144] Tao Han and JoAnne L. Hewett. Top charm associated production in high-energy e^+e^- collisions. *Phys.Rev.*, D60:074015, 1999, hep-ph/9811237.

[145] CMS Collaboration. Measurement of the ratio b(t to wb)/b(t to wq). Technical Report CMS-PAS-TOP-12-035, CERN, Geneva, 2013.

[146] J.A. Aguilar-Saavedra and A. Onofre. Using single top rapidity to measure V_td, V_ts, V_tb at hadron colliders. *Phys.Rev.*, D83:073003, 2011, 1002.4718.

[147] Stephen P. Martin. A Supersymmetry primer. 1997, hep-ph/9709356.

[148] Martin Schmaltz and David Tucker-Smith. Little Higgs review. *Ann.Rev.Nucl.Part.Sci.*, 55:229–270, 2005, hep-ph/0502182.

[149] Maxim Perelstein. Little Higgs models and their phenomenology. *Prog.Part.Nucl.Phys.*, 58:247–291, 2007, hep-ph/0512128.

[150] Hooman Davoudiasl, Shrihari Gopalakrishna, Eduardo Ponton, and Jose Santiago. Warped 5-Dimensional Models: Phenomenological Status and Experimental Prospects. *New J.Phys.*, 12:075011, 2010, 0908.1968.

[151] Roberto Contino. The Higgs as a Composite Nambu-Goldstone Boson. 2010, 1005.4269.

[152] Y. Gershtein, M. Luty, M. Narain, L. T. Wang, D. Whiteson, et al. New Particles Working Group Report of the Snowmass 2013 Community Summer Study. 2013, arXiv:1311.0299.

[153] ATLAS Collaboration. Search for direct production of the top squark in the all-hadronic ttbar + etmiss final state in 21 fb-1 of p-pcollisions at sqrt(s)=8 TeV with the ATLAS detector. *ATLAS-CONF-2013-024*, 2013.

[154] CMS Collaboration. Search for top-squark pair production in the single lepton final state in pp collisions at 8 TeV. *CMS-PAS-SUS-13-011*, 2013.

[155] CMS Collaboration. Projected Performance of an Upgraded CMS Detector at the LHC and HL-LHC: Contribution to the Snowmass Process. 2013, arXiv:1307.7135 and SNOW13-00086.

[156] Tilman Plehn, Michael Spannowsky, Michihisa Takeuchi, and Dirk Zerwas. Stop Reconstruction with Tagged Tops. *JHEP*, 1010:078, 2010, 1006.2833.

[157] Tilman Plehn, Michael Spannowsky, and Michihisa Takeuchi. Stop searches in 2012. *JHEP*, 1208:091, 2012, 1205.2696.

[158] David E. Kaplan, Keith Rehermann, and Daniel Stolarski. Searching for Direct Stop Production in Hadronic Top Data at the LHC. *JHEP*, 1207:119, 2012, 1205.5816.

[159] Bhaskar Dutta, Teruki Kamon, Nikolay Kolev, Kuver Sinha, and Kechen Wang. Searching for Top Squarks at the LHC in Fully Hadronic Final State. *Phys.Rev.*, D86:075004, 2012, 1207.1873.

[160] Daniel Stolarski. Reach in All Hadronic Stop Decays: A Snowmass White Paper. 2013, 1309.1514.

[161] Zhenyu Han and Andrey Katz. Stealth Stops and Spin Correlation: A Snowmass White Paper. 2013, 1310.0356.

[162] Can Kilic and Brock Tweedie. Cornering Light Stops with Dileptonic mT2. *JHEP*, 1304:110, 2013, 1211.6106.

[163] Andres G. Delannoy, Bhaskar Dutta, Alfredo Gurrola, Will Johns, Teruki Kamon, et al. Probing Supersymmetric Dark Matter and the Electroweak Sector using Vector Boson Fusion Processes: A Snowmass Whitepaper. 2013, arXiv:1308.0355.

[164] Christopher Brust, Andrey Katz, Scott Lawrence, and Raman Sundrum. SUSY, the Third Generation and the LHC. *JHEP*, 1203:103, 2012, 1110.6670.

[165] ATLAS Collaboration. Search for strong production of supersymmetric particles in final states with missing transverse momentum and at least three b-jets using 20.1 fb^{-1} of pp collisions at sqrt(s) = 8 TeV with the ATLAS Detector. *ATLAS-CONF-2013-061*, 2013.

[166] CMS Collaboration. Search for Supersymmetry in pp collisions at 8 TeV in events with a single lepton, multiple jets and b-tags. *CMS-PAS-SUS-13-007*, 2013.

[167] Joshua Berger, Maxim Perelstein, Michael Saelim, and Andrew Spray. Boosted Tops from Gluino Decays. 2011, 1111.6594.

[168] M Perelstein and M Saelim. Boosted tops from Gluino Decays at LHC-14. *Snowmass white paper, in preparation*, 2013.

[169] M.L. Graesser and J. Shelton. Asymmetric Stop Decays and Topness at the 14 TeV LHC. *Snowmass white paper, in preparation*, 2013.

[170] Michael L. Graesser and Jessie Shelton. Hunting Asymmetric Stops. 2012, 1212.4495.

[171] Bhaskar Dutta, Teruki Kamon, Nikolay Kolev, Kuver Sinha, Kechen Wang, et al. Top Squark Searches Using Dilepton Invariant Mass Distributions and Bino-Higgsino Dark Matter at the LHC. *Phys.Rev.*, D87:095007, 2013, 1302.3231.

[172] N. Arkani-Hamed, A. Delgado, and G.F. Giudice. The Well-tempered neutralino. *Nucl.Phys.*, B741:108–130, 2006, hep-ph/0601041.

[173] Emanuel Nikolidakis and Christopher Smith. Minimal Flavor Violation, Seesaw, and R-parity. *Phys.Rev.*, D77:015021, 2008, 0710.3129.

[174] Csaba Csaki, Yuval Grossman, and Ben Heidenreich. MFV SUSY: A Natural Theory for R-Parity Violation. *Phys.Rev.*, D85:095009, 2012, 1111.1239.

[175] Daniel Duggan, Jared A. Evans, James Hirschauer, Ketino Kaadze, David Kolchmeyer, et al. Sensitivity of an Upgraded LHC to R-Parity Violating Signatures of the MSSM. 2013, 1308.3903.

[176] Joshua Berger, Maxim Perelstein, Michael Saelim, and Philip Tanedo. The Same-Sign Dilepton Signature of RPV/MFV SUSY. *JHEP*, 1304:077, 2013, 1302.2146.

[177] Michael Saelim and Maxim Perelstein. RPV SUSY with Same-Sign Dileptons at LHC-14. 2013, 1309.7707.

[178] J. de Favereau, C. Delaere, P. Demin, A. Giammanco, V. Lematre, et al. DELPHES 3, A modular framework for fast simulation of a generic collider experiment. 2013, 1307.6346.

[179] Zhenyu Han, Andrey Katz, Minho Son, and Brock Tweedie. Boosting Searches for Natural SUSY with RPV via Gluino Cascades. 2012, 1211.4025.

[180] A. Katz. Search for RPV Gluino in RPV Natural SUSY. *Snowmass white paper, in preparation*, 2013.

[181] Jan Mrazek and Andrea Wulzer. A Strong Sector at the LHC: Top Partners in Same-Sign Dileptons. *Phys.Rev.*, D81:075006, 2010, 0909.3977.

[182] Kaustubh Agashe, Roberto Contino, Leandro Da Rold, and Alex Pomarol. A Custodial symmetry for Zb anti-b. *Phys.Lett.*, B641:62–66, 2006, hep-ph/0605341.

[183] CMS Collaboration. Inclusive search for a vector-like T quark by CMS. Technical Report CMS-PAS-B2G-12-015, 2013.

[184] ATLAS Collaboration. Search for pair production of heavy top-like quarks decaying to a high-p_{T} W boson and a b quark in the lepton plus jets final state in pp collisions at $\sqrt{s} = 8$ TeV with the ATLAS detector. Technical Report ATLAS-CONF-2013-060, Jun 2013.

[185] A. Avetisyan et al. Snowmass Energy Frontier Simulations and Performance). 2013, 1308.0843, SNOW13-00138.

[186] Aram Avetisyan, John M. Campbell, Timothy Cohen, Nitish Dhingra, James Hirschauer, et al. Methods and Results for Standard Model Event Generation at $\sqrt{s} = 14$ TeV, 33 TeV and 100 TeV Proton Colliders (A Snowmass Whitepaper). 2013, 1308.1636.

[187] A. Avetisyan, S. Bhattacharya, M. Narain, S. Padhi, J. Hirschauer, et al. Snowmass Energy Frontier Simulations using the Open Science Grid (A Snowmass 2013 whitepaper). 2013, arXiv:1308.0843, SNOW13-00168.

[188] Saptaparna Bhattacharya, Jimin George, Ulrich Heintz, Ashish Kumar, Meenakshi Narain, et al. Prospects for a Heavy Vector-Like Charge 2/3 Quark T search at the LHC with $\sqrt{s} = 14$ TeV and 33 TeV. A Snowmass 2013 Whitepaper. 2013, 1309.0026.

[189] Tim Andeen, Clare Bernard, Kevin Black, Taylor Childres, Lidia Dell'Asta, et al. Sensitivity to the Single Production of Vector-Like Quarks at an Upgraded Large Hadron Collider. 2013, 1309.1888.

[190] Erich W. Varnes. Vector-like B pair production at future pp colliders. 2013, 1309.0788.

[191] Roberto Contino and Geraldine Servant. Discovering the top partners at the LHC using same-sign dilepton final states. *JHEP*, 0806:026, 2008, 0801.1679.

[192] Aram Avetisyan and Tulika Bose. Search for top partners with charge 5e/3. 2013, 1309.2234.

[193] Robert M. Harris, Christopher T. Hill, and Stephen J. Parke. Cross-section for topcolor Z-prime(t) decaying to t anti-t: Version 2.6. 1999, hep-ph/9911288.

[194] ATLAS Collaboration. A search for ttbar resonances in the lepton plus jets final state with ATLAS using 4.7 fb^{-1} of pp collisions at sqrt(s) = 7 TeV. 2013, 1305.2756.

[195] CMS Collaboration. Search for $t\bar{t}$ resonances in semileptonic final states in pp collisions at $\sqrt{s} = 8$ TeV. *CMS-PAS-B2G-12-006*, 2013.

[196] ATLAS Collaboration. Search for resonances decaying into top-quark pairs using fully hadronic decays in pp collisions with ATLAS at $\sqrt{s} = 7$ TeV. *JHEP*, 1301:116, 2013, 1211.2202.

[197] CMS Collaboration. Search for anomalous top quark pair production in the boosted all-hadronic final state using pp collisions at $\sqrt{s} = 8$ TeV. *CMS-PAS-B2G-12-005*, 2013.

[198] Kaustubh Agashe, Alexander Belyaev, Tadas Krupovnickas, Gilad Perez, and Joseph Virzi. LHC Signals from Warped Extra Dimensions. *Phys.Rev.*, D77:015003, 2008, hep-ph/0612015.

[199] Vernon Barger, Tao Han, and Devin G.E. Walker. Top Quark Pairs at High Invariant Mass: A Model-Independent Discriminator of New Physics at the LHC. *Phys.Rev.Lett.*, 100:031801, 2008, hep-ph/0612016.

[200] Ia Iashvili, Supriya Jain, Avto Kharchilava, and Harrison B. Prosper. Discovery potential for heavy t-tbar resonances in dilepton+jets final states. 2013, 1309.7684.

[201] Kaustubh Agashe, Oleg Antipin, Mihailo Backovic, Aaron Effron, Alex Emerman, et al. Warped Extra Dimensional Benchmarks for Snowmass 2013. 2013, 1309.7847.

[202] Leandro G. Almeida, Seung J. Lee, Gilad Perez, George Sterman, and Ilmo Sung. Template Overlap Method for Massive Jets. *Phys.Rev.*, D82:054034, 2010, 1006.2035.

[203] Mihailo Backovic, Jose Juknevich, and Gilad Perez. Boosting the Standard Model Higgs Signal with the Template Overlap Method. 2012, 1212.2977.

[204] ATLAS Collaboration. Search for tb resonances in proton-proton collisions at $\sqrt{s} = 7$ TeV with the ATLAS detector. *Phys.Rev.Lett.*, 109:081801, 2012, 1205.1016.

[205] ATLAS Collaboration. Search for $W' \to t\bar{b}$ in proton-proton collisions at a centre-of-mass energy of $\sqrt{s} = 8$ TeV with the ATLAS detector. Technical Report ATLAS-CONF-2013-050, CERN, Geneva, May 2013.

[206] CMS Collaboration. Search for a W' boson decaying to a bottom quark and a top quark in pp collisions at $\sqrt{s} = 7$ TeV. *Phys.Lett.*, B718:1229–1251, 2013, 1208.0956.

[207] Elizabeth Drueke, Brad Schoenrock, Barbara Alvarez Gonzalez, and Reinhard Schwienhorst. Searches for resonances in the tb and tc final states at the high-luminosity LHC. 2013, 1309.7043.

[208] Priscila M. Aquino, Gustavo Burdman, and Oscar J.P. Eboli. A Signal for a theory of flavor at the LHC. *Phys.Rev.Lett.*, 98:131601, 2007, hep-ph/0612055.

[209] M. Artuso, M. Papucci, and S. Prell. Flavor Mixing and CP Violation at High Energy. *Snowmass whitepaper, in preparation*, 2013.

[210] Joseph Nutter, Reinhard Schwienhorst, Devin G.E. Walker, and Jiang-Hao Yu. Single Top Production as a Probe of B-prime Quarks. *Phys.Rev.*, D86:094006, 2012, 1207.5179.

[211] ATLAS Collaboration. Search for single b^*-quark production with the ATLAS detector at $\sqrt{s} = 7$ TeV. *Phys.Lett.*, B721:171–189, 2013, 1301.1583.

[212] R. Calkins, Chekanov S., Dolen J., Pilot J., Pöschl R., and Tweedie. B. Reconstructing top quarks at the upgraded LHC and at future accelerators (Summary of "Top algorithms and detectors" High Energy Frontier Study Group). 2013, arXiv:1307.6908, SNOW13-00076.

[213] S. Ovyn, X. Rouby, and V. Lemaitre. DELPHES, a framework for fast simulation of a generic collider experiment. 2009, 0903.2225.

[214] Matteo Cacciari, Gavin P. Salam, and Gregory Soyez. The anti-k_t jet clustering algorithm. *JHEP*, 04:063, 2008, 0802.1189.

[215] ATLAS Collaboration. Measurement of the top quark mass from 2011 ATLAS data using the template method. Technical Report ATLAS-CONF-2011-120, CERN, Geneva, Aug 2011.

[216] A. Abdesselam, E. Bergeaas Kuutmann, U. Bitenc, G. Brooijmans, J. Butterworth, et al. Boosted objects: A Probe of beyond the Standard Model physics. *Eur.Phys.J.*, C71:1661, 2011, 1012.5412.

[217] A. Altheimer, S. Arora, L. Asquith, G. Brooijmans, J. Butterworth, et al. Jet Substructure at the Tevatron and LHC: New results, new tools, new benchmarks. *J.Phys.*, G39:063001, 2012, 1201.0008.

[218] Stephen D. Ellis, Christopher K. Vermilion, and Jonathan R. Walsh. Recombination Algorithms and Jet Substructure: Pruning as a Tool for Heavy Particle Searches. 2009, 0912.0033.

[219] Stephen D. Ellis, Christopher K. Vermilion, and Jonathan R. Walsh. Techniques for improved heavy particle searches with jet substructure. *Phys. Rev.*, D 80:051501, 2009, 0903.5081.

[220] David Krohn, Jesse Thaler, and Lian-Tao Wang. Jet Trimming. *JHEP*, 1002:084, 2010, 0912.1342.

[221] Jonathan M. Butterworth, Adam R. Davison, Mathieu Rubin, and Gavin P. Salam. Jet substructure as a new higgs search channel at the lhc. *Phys. Rev. Lett.*, 100:242001, 2008.

[222] Ben Lillie, Lisa Randall, and Lian-Tao Wang. The Bulk RS KK-gluon at the LHC. *JHEP*, 09:074, 2007, hep-ph/0701166.

[223] J. M. Butterworth, John R. Ellis, and A. R. Raklev. Reconstructing sparticle mass spectra using hadronic decays. *JHEP*, 05:033, 2007, hep-ph/0702150.

[224] Leandro G. Almeida, Seung J. Lee, Gilad Perez, Ilmo Sung, and Joseph Virzi. Top Jets at the LHC. *Phys. Rev.*, D 79:074012, 2009, 0810.0934.

[225] Leandro G. Almeida et al. Substructure of high-p_T Jets at the LHC. *Phys. Rev.*, D 79:074017, 2009, 0807.0234.

[226] David E. Kaplan, Keith Rehermann, Matthew D. Schwartz, and Brock Tweedie. Top Tagging: A Method for Identifying Boosted Hadronically Decaying Top Quarks. *Phys. Rev. Lett.*, 101:142001, 2008, 0806.0848.

[227] Gustaaf H Brooijmans. High pT Hadronic Top Quark Identification. Published in "A Les Houches Report. Physics at Tev Colliders 2007 – New Physics Working Group", 2008, hep-ph/0802.3715.

[228] Jonathan M. Butterworth et al. Discovering baryon-number violating neutralino decays at the LHC. Technical Report CERN-PH-TH/2009-073, hep-ph/0906.0728, 2009.

[229] ATLAS Collaboration. Reconstruction of high mass $t\bar{t}$ resonances in the lepton+jets channel. Technical Report ATL-PHYS-PUB-2009-081, CERN, Geneva, May 2009.

[230] CMS Collaboration. A Cambridge-Aachen (C-A) based Jet Algorithm for boosted top-jet tagging. Technical Report CMS-PAS-JME-09-001, CERN, 2009.

[231] Christoph Hackstein and Michael Spannowsky. Boosting Higgs discovery - the forgotten channel, 2010, 1008.2202.

[232] S. Chekanov and J. Proudfoot. Searches for TeV-scale particles at the LHC using jet shapes. *Phys. Rev.*, D81:114038, 2010.

[233] S. V. Chekanov, C. Levy, J. Proudfoot, and R. Yoshida. New approach for jet-shape identification of TeV-scale particles at the LHC. *Phys. Rev.*, D82:094029, 2010.

[234] ATLAS Collaboration. Prospects for top anti-top resonance searches using early ATLAS data. Technical Report ATL-PHYS-PUB-2010-008, CERN, Geneva, Jul 2010.

[235] Jesse Thaler and Ken Tilburg. Identifying boosted objects with n-subjettiness. *Journal of High Energy Physics*, 2011(3):1–28, 2011.

[236] ATLAS Collaboration. Performance of jet substructure techniques for large-R jets in proton-proton collisions at $\sqrt{s} = 7$ TeV using the ATLAS detector. 2013, 1306.4945.

[237] ATLAS Collaboration. Jet mass and substructure of inclusive jets in $\sqrt{s} = 7$ TeV pp collisions with the ATLAS experiment. *JHEP*, 1205:128, 2012, 1203.4606.

[238] ATLAS Collaboration. A search for $t\bar{t}$ resonances in lepton+jets events with highly boosted top quarks collected in pp collisions at $\sqrt{s} = 7$ TeV with the ATLAS detector. *JHEP*, 1209:041, 2012, 1207.2409.

[239] M.J. Oreglia. A Study of the Reactions psi prime to gamma gamma psi,. Ph.D. Thesis, SLAC-R-236, 1980.

[240] S. Catani, Yuri L. Dokshitzer, M. H. Seymour, and B. R. Webber. Longitudinally invariant K_t clustering algorithms for hadron hadron collisions. *Nucl. Phys.*, B406:187–224, 1993.

[241] Stephen D. Ellis and Davison E. Soper. Successive combination jet algorithm for hadron collisions. *Phys. Rev.*, D48:3160–3166, 1993, hep-ph/9305266.

[242] L. Weuste and F. Simon. Mass and cross section measurements of light-flavored squarks at clic. Aug 2011.

[243] ATLAS Collaboration. Jet energy resolution in proton-proton collisions at $\sqrt{s} = 7$ TeV recorded in 2010 with the ATLAS detector. *Eur.Phys.J.*, C73:2306, 2013, 1210.6210.